AN ABSTRACT OF THE THESIS OF

Adrian F. Gombart for the degree of Master of Science in Genetics presented on May 8, 1989.

TITLE: OpMNPV p32, a Baculovirus Polyhedral Envelope-Associated Protein: Genetic Location, Nucleotide Sequence, Transcriptional Mapping and Immunocytochemical Characterization

Abstract approved:

George F. Rohrmann

Baculoviruses comprise a diverse group of pathogens infectious for members of the insect orders Lepidoptera, Hymenoptera and Diptera. Of the three subgroups, two (subgroup A, nuclear polyhedrosis virus (NPV) and subgroup B, granulosis virus (GV) are occluded in a crystalline protein structure while the remaining subgroup (subgroup C, non-occluded virus) is not. These viruses have a large double-stranded, supercoiled DNA genome (88-160 kb) packaged within a rod-shaped, enveloped nucleocapsid. Two viral phenotypes are observed during the life cycle of the virus. The polyhedra-derived virus (PDV) is packaged in polyhedra within the cell nucleus late in infection and is responsible for primary infection of the insect. The nucleocapsid of the budded virus (BV) is assembled in the nucleus and acquires an envelope as it is budded from the cell early in infection. This form of the virus is responsible for spread of infection from cell to cell in the insect. Very few baculovirus structural proteins have been well characterized as to their genetic location, expression and function. Characterization of viral and virally-associated structural proteins will lead to a better understanding of virus structure and function and determination of phenotype specific proteins will allow a better understanding of phenotype regulation. The purpose of this study was to determine the genetic location of a structural protein and charcterize its expression and location during infection and possibly elucidate its function.

Using a polyclonal mouse antiserum produced against purified virions of the multicapsid nuclear polyhedrosis virus of Orgyia

pseudotsugata (OpMNPV), I identified two immunoreactive lambda gtll clones containing non-overlapping insert DNAs which mapped to a single open reading frame (ORF) in the HindIII-M fragment. Analysis of nucleotide sequence data indicates that this ORF encodes a protein with a MW of 32.4 kDa. A trpE-p32 gene fusion containing the entire p32 ORF was constructed, and the fusion protein was purified and used to immunize rabbits. Western blot analysis and immunofluorescence studies using the anti-TrpE-p32 antiserum detected a polyhedra-derived virus (PDV)-associated protein of 32 kDa at 24 hours post infection (hpi). The protein was observed in the cytoplasm and nucleus at 24 hpi and became concentrated in the cytoplasm late in infection. Western blot analysis and immunofluorescent microscopy of polyhedra solubilized under various conditions, indicated that p32 is associated with the polyhedral envelope. The predicted amino acid sequence for p32 showed 58% amino acid identity with the predicted amino acid sequence for an ORF (ORF 3) in a similar region of the genome of the MNPV of Autographa californica (AcMNPV) (Oellig et al., 1987). The solubility properties of the p32 protein and reciprocal immunoblotting experiments indicate the OpMNPV p32 gene encodes a protein which is homologous to the polyhedral envelope-associated phosphoprotein, pp34, recently reported by Whitt and Manning (1988).

In addition, the sequenced HindIII-M region of the OpMNPV genome was transcriptionally mapped and compared to the homologous region in the AcMNPV genome. Five ORFs (including the above mentioned ORF 3) were identified and compared between AcMNPV and OpMNPV and amino acid homologies of 25-70% were observed. The comparison revealed a number of major differences in the genomes of the two viruses. Discontinuous homology between the two viruses of the ORF 1 gene led to the identification of a putative transposable element in the AcMNPV ORF 1 sequence reported by Oellig et al (1987). In addition, it was found that a region corresponding to the 4 kb HindIII-K/EcoRl-S region of AcMNPV was not present in the OpMNPV genome. Although the ORFs characterized in the OpMNPV HindIII-M region all were expressed as late genes and all contained the conserved ATAAG putative promoter/mRNA start site sequence,

primer extension analysis indicated that use of this signal for transciptional initiation may vary between different ORFs.

OpMNPV p32, a Baculovirus Polyhedral Envelope-Associated Protein: Genetic Location, Nucleotide Sequence, Transcriptional Mapping and Immunocytochemical Characterization

by

Adrian F. Gombart

A THESIS

submitted to

Oregon State University

in partial fulfillment of
the requirements for the
degree of

Master of Science

Completed May 8, 1989

Commencement June, 1990

APPROVED:

Redacted for Privacy

Professor of Agricultural Chemistry in charge of major

Redacted for Privacy

Chairman of Genetics

Redacted for Privacy

Dean of Graduate School

Date thesis is presented May 8, 1989

Typed by Adrian Gombart for Adrian F. Gombart

PREFACE

Contributions of coauthors to the work in the chapters following:

Dr. George F. Rohrmann provided lab space and funding for the duration of the project. As the major professor and primary investigator, he also provided guidance and co-wrote and edited parts of chapters II and III.

Dr. George S. Beaudreau provided lab space and funding for the duration of the project. He also assisted with the immunofluorescenct microscopy portion of chapter II.

Dr. Margot N. Pearson produced the polyclonal antiserum against the purified OpMNPV virions and screened and isolated the two lambda gtll clones (chapter II) containing the inserts from the p32 gene.

Dr. Gary W. Blissard isolated the total RNA and poly(A+) RNA used in the transcriptional mapping experiments performed in chapter III. He assisted in the primer extension and S1 analysis experiments in chapter III and also provided his computer and talents in the production of the line figures.

ACKNOWLEDGEMENTS

Chapter 2: I thank Dr. Loy Volkman for performing the reciprocal Western blots on AcMNPV and OpMNPV PDV with our anti-TrpE-p32 antiserum and her monoclonal antibody to pp34 and Mary Bradford for her excellent work on the dissolution studies of OpMNPV polyhedra proteins. I would like to thank Rebecca Quant-Russell and Dr. Gary Blissard for their valuable technical advice and Christian Gross for critically reading this manuscript. I also would like to thank Jack Kramer of the Center for Gene Research and Biotechnology at OSU for producing the hydropathy plots. This project was supported by grants from the USDA (87-CRCR-1-2380) and the NIH (AI 21983).

Chapter 3: I thank Dr. Peter Faulkner for making available AcMNPV sequence data prior to its publication. I also would like to thank Rebecca Quant-Russell and Dr. Margot Pearson for their valuable technical advice and Christian Gross for critically reading this manuscript. I also thank Jack Kramer and Reg McParland of the Center for Gene Research and Biotechnology at OSU for assistance with DNA sequence analysis and primer synthesis. This project was supported by grants from the USDA (87-CRCR-1-2380) and the NIH (AI 21983).

I would like to thank the following people who have been of great asssistance during my graduate career at OSU: Dr. George S. Beaudreau and Dr. George F. Rohrmann, my major professor, for allowing me to perform my thesis work in their laboratory and for their invaluable advice and guidance; Rebecca Quant-Russell, Dr. Margot Pearson and Dr. Gary Blissard to whom I am indebted for teaching me the majority of the techniques used during the course of this project; Dr. George Pearson (Chairman of the Genetics Program at OSU) for his assistance in cutting through the multitude of "red tape" on my way to a Master's degree and excellent advice; Dr. Christopher Mathews (Chairman of the Department of Biochemistry and Biophysics) for taking time out of his busy schedule to serve on my committee as minor professor; my fellow graduate students Christian Gross, Mary Bradford and Rolf Muller for their advice and friendship

and, of course, my family and friends for their support and interest in my work.

TABLE OF CONTENTS

LIST OF FIGURES

LIST OF TABLES

Chapter III

OpMNPV p32, A BACULOVIRUS POLYHEDRAL ENVELOPE-ASSOCIATED PROTEIN: GENETIC LOCATION, NUCLEOTIDE SEQUENCE, TRANSCRIPTIONAL MAPPING AND IMMUNOCYTOCHEMICAL CHARACTERIZATION

Chapter 1

INTRODUCTION

Baculoviridae are a family of pathogens infectious for the insect orders of Lepidoptera, Hymenoptera and Diptera. They are composed of three subgroups. Subgroup A, the nuclear polyhedrosis viruses (NPVs) and Subgroup B, the granulosis viruses (GVs), both occlude their virions in large protein crystals to form occlusion bodies (OBs). Subgroup C baculoviruses are non-occluded. The GVs usually only have a single virion per cytoplasmic crystal while the NPVs have many virions occluded within a single intranuclear crystal (for a review see Vlak and Rohrmann, 1985). The NPVs are comprised of two morphological types. In the first type, many single, enveloped nucleocapsids (SNPVs) are occluded within the OBs and in the second type, one or more nucleocapsids within one envelope (MNPV) are occluded (Granados, 1980). Baculoviruses have a large, double-stranded, supercoiled DNA genome which ranges from 88-153 kilobases (kb) in size (Burgess, 1977; Schafer et al., 1979). The genome is packaged within a protein capsid which together are known as the nucleocapsid. The nucleocapsid is enveloped in a "unit" membrane and is, in turn, occluded in a paracrystalline protein matrix composed primarily of the protein polyhedrin (Vlak and Rohrmann, 1985). The OB is enclosed in an electron-dense, amorphous, polyhedral envelope which is composed predominantly of carbohydrate (Minion et al., 1979). Until recently, it was not known whether proteins were associated with this envelope. Whitt and Manning (1988) demonstrated that a 34 kDA phosphoprotein is associated with the polyhedral membrane of the MNPV infectious for Autographa californica (AcMNPV).

The virus exists in the environment in the occluded form

protected by the polyhedrin crystal. The virus is normally ingested by the insect. As the NPV-OBs pass into the midgut lumen, the virions are released upon dissolution of the crystalline matrix by the alkaline surroundings of the insect midgut. The released virions pass through the peritropic membrane and come into contact with the microvilli of the columnar cells (for a review see Granados, 1980). The virus enters the cell by fusion of the virus envelope with the microvillus of the plasma membrane. The virus uncoats at the nuclear membrane while the nucleocapsid is observed in the cytoplasm peripheral to the nucleus and aligned at right angles to the nuclear pores (Summers, 1971). The virus replicates within the nucleus and produces two distinct viral phenotypes. The budded virus (BV), which is produced early in infection by budding of the nucleocapsid through the plasma membrane, is responsible for the spread of infection within the insect. The second form, the occluded form (or polyhedra-derived virus), is produced later in infection and is responsible for primary infection of the insect.

Various studies have demonstrated that a degree of sequence homology is present among the various genomes of baculoviruses. Initially it was observed by DNA-DNA hybridization studies that the MNPV of Orgyia psuedotsugata (OpMNPV) and AcMNPV possessed over 24% sequence homology under non-stringent annealing conditions (Rohrmann et al., 1982). More recently, the genomes of these two viruses were shown to be colinearly organized (Leisy et al., 1984), however, the absence of homologous repeat sequences in OpMNPV, which have been implicated as enhancers of delayed early genes in AcMNPV, was demonstrated by Bicknell et al. (1987). Comparison of nucleotide sequences of similar regions between the two viruses has demonstrated a wide range of homologies between OpMNPV and AcMNPV (Leisy et al., 1986; Rohrmann, 1986; Bicknell et al., 1987). Of all the genes studied to date, the polyhedrin gene shows the highest degree of homology among various baculoviruses (for a review see Rohrmann, 1986).

Transcription of baculovirus genes has been found to be very complex. At early times postinfection, transcription occurs at

dispersed regions of the genome, however, at late times postinfection transcription occurs at loci throughout the genome (Erlandson and Carstens, 1983). At least three and perhaps four general classes of genes are expressed from the AcMNPV genome: immediate early, delayed early, late, and very late (for a review see Friesen and Miller, 1986). Various overlapping arrangements have been observed for transcripts including those with coterminal 5′ ends and extended 3′ ends and those with various 5′ends and coterminal 3′ ends (Friesen and Miller, 1985; Lubbert and Doerfler, 1984 a and b; Oellig et al., 1987; Rankin et al., 1986). These overlapping transcripts differ in their temporal expression. The complexity of baculovirus transcription has been suggested to compensate for the lack of RNA splicing in the genome (Lubbert and Doerfler, 1984 b). Recently, however, splicing has been observed in the immediate early IE-1 gene (Chisholm and Henner, 1988). The complexity of transcription may be related to the regulation of gene expression by mechanisms such as promoter occlussion (Friesen and Miller, 1985), antisense RNA translated inhibition (Friesen and Miller, 1987) or polycistronic translation (Kozak, 1986; Oellig et al., 1987). The consensus sequence ATAAG found upstream of all late expressed genes (Rohrmann, 1986) has been suggested to be important in either initiation of or specificity of (or both) transcription (Rohrmann, 1986; Possee and Howard, 1987). Apparently the TATA and CAAT consensus sequences are important in the transcription of other classes of genes.

Few viral structural proteins have been well characterized as to their genetic location, expression and function. Of the proteins characterized thus far, four have been found to be associated with the NPV virions and two associated with polyhedra. The four proteins associated with NPV virions are p10, p6.9, p39 and gp64. p10 has been sequenced and transcriptionally mapped in both OpMNPV and AcMNPV (Leisy et al., 1986; Kuzio et al., 1984; Rankin et al., 1986). The protein has been found to be hyperexpressed late in infection and to be associated with PDV in OpMNPV (Quant-Russell et al., 1987). Immunofluorescence studies using monoclonal antibodies

against OpMNPV p10 indicate that p10 forms intensely staining cytoplasmic structures in OpMNPV-infected Lymantria dispar cells (Quant-Russell et al., 1987). Also, a reaction of the p10 antiserum with the cytoskeleton of uninfected cells was observed. Electron microscopy studies using rabbit antibodies against AcMNPV p10 demonstrated that p10 is found specifically associated with fibrous-like structures in the nucleus and cytoplasm of AcMNPV infected cells (Van der Wilk et al., 1987). The function of p10 is not known, however, these studies suggest it may have an important role in the development of polyhedra. p6.9 has been sequenced and transcriptionally mapped (Wilson, et al., 1987). The predicted amino acid sequence shows it to be an arginine-rich polypeptide which appears to be phosphorylated during the uncoating process within the nucleus. p6.9 has been hypothesized to be a DNA binding protein (Wilson et al., 1987). The OpMNPV p39 was recently sequenced and transcriptionally mapped (Blissard et al., 1989). Immunoblot studies using a series of monoclonal antibodies against p39 indicated that the protein was expressed late in infection of OpMNPV-infected L. dispar cells and p39 is associated with both the PDV and BV (Pearson et al., 1988). Immunofluorescent microscopy studies indicated that the protein is detected primarily in the nucleus and one of the monoclonal antibodies crossreacted with a host cell protein associated with the condensed chromosomes present during mitosis (Pearson et al., 1988). The function of this protein has not been determined. A fourth NPV protein is a 64 kDa glycoprotein found predominantly with the budded form of the virus (for a reveiw see Volkman, 1986). Evidence from light and electron microscopic studies indicate that gp64 is an envelope protein. It is present in the plasma membrane of infected cells before virus budding. The BV envelopes stain predominantly at the location of the peplomers (Volkman et al., 1984). A monoclonal antibody (AcV_1) has been found to neutralize BV infectivity (Volkman and Goldsmith, 1985). gp64 is believed to compose the viral peplomers and apparently plays a role in the penetration step of BV infection.

The two structural proteins associated with polyhedra are

polyhedrin and pp34 (p32 in OpMNPV). Polyhedrin is the major component of the crystalline protein matrix surrounding the enveloped nucleocapsids in polyhedra. pp34 is a phosphoprotein of AcMNPV and it was recently demonstrated to be thiolly linked to the carbohydrate layer surrounding the polyhedra (Whitt and Manning, 1988).

Our laboratory has undertaken a systematic approach to identify and characterize baculovirus structural proteins. Monoclonal antibodies produced against polyhedra-derived virus have been used both to characterize the expression of proteins using immunoblots and immunofluorescence analyses and to locate the genes encoding the proteins by screening a lambda gtll expression library of OpMNPV DNA (Quant-Russell et al., 1987; Pearson et al., 1988). In chapter 2 of this report, we describe the use of a polyclonal mouse antiserum produced against PDV proteins to screen a lambda gtll library. Two immunoreactive clones contained insert DNA from an open reading frame (one of five) in the HindIII-M region encoding a 32 kDa protein. Antisera was produced against a fusion protein containing the entire p32 open reading frame (ORF) and was used to characterize a 32 kDa protein which is found associated with the polyhedral envelope of OpMNPV. In chapter 3, we describe the nucleotide sequence and transcriptional organization of the HindIII-M region of OpMNPV. Comparison of the OpMNPV nucleotide and predicted amino acid sequences to those for the homologous region in AcMNPV (Oellig et al., 1987) indicated that, in addition to lacking an hr enhancer sequence, there is the insertion of a transposable element into the AcMNPV ORF 1 sequence. Also, a region homologous to the 4 kb HindIII-K/EcoR1-S which is located between the ORF 5 and p26 genes of AcMNPV, is not present in OpMNPV. The significance of these differences is discussed.

Chapter II

A Baculovirus Polyhedral Envelope-Associated Protein: Genetic Location, Nucleotide Sequence and Immunocytochemical Characterization

by

Adrian F. Gombart, George F. Rohrmann, Margot N. Pearson, and George S. Beaudreau

Oregon State University

Department of Agricultural Chemistry

May 8, 1989

Published: Virology 169, 182-193 (1989)

Chapter II

A Baculovirus Polyhedral Envelope-Associated Protein: Genetic Location, Nucleotide Sequence, and Immunocytochemical Characterization

ABSTRACT

Using a polyclonal mouse antiserum produced against purified virions of the multicapsid nuclear polyhedrosis virus of *Orgyia pseudotsugata* (OpMNPV), we identified two immunoreactive lambda gtll clones containing non-overlapping insert DNAs which mapped to a single open reading frame (ORF) in the HindIII-M fragment. Analysis of nucleotide sequence data indicates that this ORF encodes a protein with a MW of 32.4 kDa. A *trpE*-p32 gene fusion containing the entire p32 ORF was constructed, and the fusion protein was purified and used to immunize rabbits. Western blot analysis and immunofluorescence studies using the anti-TrpE-p32 antiserum detected a polyhedra-derived virus (PDV)-associated protein of 32 kDa at 24 hours post infection (hpi). The protein was observed in the cytoplasm and nucleus at 24 hpi and became highly concentrated in the cytoplasm late in infection. Western blot analysis and immunofluorescent microscopy of polyhedra dissociated and solubilized under various conditions, indicated that p32 is associated with the polyhedral envelope. The predicted amino acid sequence for p32 showed 58% amino acid identity with the predicted amino acid sequence for an ORF (ORF 3) in a similar region of the genome of the MNPV of *Autographa californica* (AcMNPV) (Oellig et al., 1987). The solubility properties of the p32 protein and reciprocal immunoblotting experiments indicate the OpMNPV p32 gene encodes a protein which is homologous to the polyhedral envelope-associated phosphoprotein, pp34, recently reported by Whitt and Manning (1988).

INTRODUCTION

The multicapsid nuclear polyhedrosis virus of *Orgyia* pseudotsugata (OpMNPV) is a member of baculovirus subgroup A (nuclear polyhedrosis viruses, NPVs). Baculoviruses have large, double-stranded, supercoiled DNA genomes packaged within a protein nucleocapsid and are enveloped either singly or in multiples in a "unit" membrane (for review see Vlak and Rohrmann, 1985). These enveloped nucleocapsids are occluded in a paracystalline protein matrix composed primarily of the protein polyhedrin. The occlusion bodies are surrounded by an electron-dense, amorphous, polyhedral envelope shown to be composed predominantly of carbohydrate (Minion et al., 1979). The occluded form (polyhedra-derived virus, PDV) of the virus is responsible for the primary infection of the insect. A second virus phenotype, the non-occluded virus or budded virus (BV), is responsible for spread of infection within the infected host insect (for review see Granados and Williams, 1986).

At present, only four structural proteins associated with NPVs have been well-characterized in terms of both their genetic location and expression. These are the proteins p10 (Leisy et al., 1986; Quant-Russell et al., 1987 and Kuzio et al., 1984) , the arginine-rich p6.9 (Wilson et al., 1987), p39 (Blissard et al., submitted and Pearson et al., in press) and gp64 (Volkman, 1986 and Dr. Gary Blissard, personal communication). To date, only two proteins other than the virion structural proteins have been found associated with polyhedra. One is polyhedrin and the other is a 34 kDa phosphoprotein which appears to be linked by thiol-glycosidic bonds to the polyhedral envelope of AcMNPV (Whitt and Manning, 1988).

We have undertaken a systematic approach to identify and characterize baculovirus structural proteins. Monoclonal antibodies produced to polyhedra-derived viral structural proteins have been used both to characterize the expression of the proteins in infected cells using Western blots and immunofluorescence analyses and to locate the genes coding for the proteins by screening a lambda gt11

expression library of OpMNPV DNA (Quant-Russell et al., 1987 and Pearson et al., in press). In this report, we describe the use of a polyclonal mouse antiserum produced against purified OpMNPV polyhedra-derived virion proteins to screen a lambda gtll expression library of OpMNPV DNA (Quant-Russell et al., 1987). Two immunoreactive clones contained insert DNA from an open reading frame (ORF) encoding a 32 kDa protein. Antisera was produced against a fusion protein containing the entire p32 ORF and was used in Western blot and immunofluorescent microscopy studies to characterize a 32 kDa protein which is found associated with the polyhedral envelope of OpMNPV.

MATERIALS AND METHODS

Insect cell lines and virus

The *Lymantria dispar* cell line and the OpMNPV used for this work and virus production, isolation and purification have been described previously (Quant-Russell et al., 1987).

Polyclonal antibody production, construction and screening of the lambda gtll library

Balb/c mice (4-6 weeks old) were immunized with sucrose gradient-purified OpMNPV polyhedra-derived virion proteins as described previously (Quant-Russell et al., 1987). Immune serum was recovered after the second boost. An OpMNPV lambda gtll expression library (Quant-Russell et al., 1987) was screened with the mouse antiserum as described by Quant-Russell et al. (1987).

Localization and nucleotide sequencing of the p32 gene

DNA inserts from lambda gtll recombinants selected by the polyclonal antiserum were isolated and used in Southern hybridization analysis (Maniatis et al., 1982) to locate the p32 gene. DNA inserts from the lambda gtll clones were excised, gel-purified, and hexamer labeled with [α-^{32}P]dATP (Feinberg and Vogelstein, 1984). The labeled lambda gtll inserts were hybridized to Southern blots of digested OpMNPV cosmid DNA (Leisy et al., 1984) and total genomic DNA. Also, these inserts were cloned into M13mp18 and the nucleotide sequence determined. Double-stranded lambda DNA sequencing of the lambda gtll clones was performed to determine the orientation of the ORF. Approximately 1-2 μg of Lambda DNA, 5X Sequenase buffer and 1 μg of "forward primer" (complementary to Lac Z sequences adjacent to the EcoRI site in lambda gtll) were mixed together and boiled for 10 min. Sequenase sequencing reactions were then immediately carried out as described by the manufacturer

(United States Biochemical). The region containing the p32 gene was sequenced using appropriate restriction enzyme fragments and exonuclease III deletion mutants produced using the method of Henikoff (1984). Both M13 and plasmid sequencing was accomplished using the dideoxy chain termination method of Sanger et al. (1980) using [α-^{35}S]dATP and the Sequenase sequencing kit (United States Biochemical). The plasmids pUC-18, pUC-19 and pBS M13 (-) (Stratagene Cloning Systems, Inc.) and the M13 phage strains mp18 and mp19 were used for cloning and sequencing. The *E. coli* host strains, HB101, JM83 and JM103, were used for plasmid production. JM103 was used for M13 phage production. Restriction enzymes and DNA modifying enzymes were purchased from Bethesda Research Laboratories, United States Biochemical, and New England Biolabs and used according to the manufacturer's instructions. All isotopes were purchased from New England Nuclear.

Construction of the *trpE*-p32 gene fusion

A pUC-19 recombinant containing the HindIII-M fragment of OpMNPV was digested with PstI and the 2.65 kilobasepair (kbp) fragment containing the entire p32 gene was isolated and purified using Gene Clean (Bio 101, Inc.). The 2.65 kbp PstI fragment was blunted with S1 nuclease, digested with SalI and the resulting 1.34 kbp fragment was ligated into M13mp18 previously digested with SmaI and SalI. DNA sequencing indicated that the S1 nuclease digested 6 basepairs (bp) beyond the PstI site. The insert containing the p32 ORF was removed from the M13 recombinant with EcoRI and HindIII and cloned into the TrpE expression vector pATH3 (similar to pATH 2 described by Dieckmann and Tzagoloff, 1985) cut with EcoRI and HindIII.

Expression, isolation and purification of TrpE-Orf3 fusion protein

Methods for induction of the fusion protein were similar to those described by Tollefson et al. (1988) and Spindler et al.

(1984). Cultures of HB101 recombinants were grown overnight in M9 media (Maniatis et al., 1982) plus 1% casamino acids, 100 μg of ampicillin per ml, and 20 μg of tryptophan (Trp) per ml and then diluted 1:10 in the same media lacking tryptophan and incubated at 30°C for 60 min. To induce the fusion protein, β-indoleacrylic acid (Sigma) was added to a final concentration of 20 μg per ml and the culture was incubated overnight at 30°C. Total cell lysates for SDS-PAGE were prepared by resuspending the cells in urea-SDS buffer (6 M urea, 1% SDS, 1% 2-mercaptoethanol, 0.01 M sodium phosphate buffer, pH 7.2) modified from Kleid et al. (1981), an equal volume of 2X reducing sample buffer (Laemmli, 1970) and boiling for 5 min. To screen the recombinants for expression of the fusion protein, the total cell lysates were electrophoresed on 9% SDS-polyacrylamide gels (Laemmli, 1970). The proteins were visualized by staining with Coomassie brilliant blue.

To extract the fusion protein for gel-isolation, cells from 100 ml of culture were resuspended in 2 ml of 50 mM Tris HCl (pH 7.5)-5 mM EDTA and 3 mg per ml lysozyme and lysed on ice for 30 min. NaCl and Nonidet P-40 (NP-40) were added to final concentrations of 0.3 M and 0.5%, respectively, and incubation on ice was continued for 30 min. The solution was then adjusted to a final concentration of 2 μg per ml DNase I and 5 mM $MgCl_2$ per ml and incubated for 60 min on ice. The sample was centrifuged at 10 K for 30 min and both the supernatant (soluble) and pellet (insoluble) portions were collected. The pellet was resuspended in 2 ml of 10 mM Tris (pH 7.5) and both fractions were stored at -80°C. The majority of the fusion protein was found in the insoluble fraction.

To isolate the fusion protein, 107 μl of the insoluble fraction (resuspended pellet) was mixed with an equal volume of 2X reducing sample buffer, boiled for 5-10 min, and electrophoresed on a 10% SDS polyacrylamide gel. The fusion protein band was visualized by staining the gel with ice cold KCl as modified from Hager and Burgess (1980), (0.1 M KCl without DTT was used for staining and destaining was not necessary). The 70 kDa band was excised and electroeluted at 200 V for 4-6 hours using a Schleicher

and Schuell Elutrap. The eluate was stored at -80°C. The amount of protein in the eluate was determined by comparison with protein standards of known concentration.

New Zealand White female rabbits were initially injected with approximately 500 μg of fusion protein emulsified in complete Freund's adjuvant. Subsequent injections of approximately 100-200 μg of fusion protein emulsified in incomplete Freund's adjuvant were given biweekly starting the third week after the intial injection. Immune serum was collected 7 days after each boost. For these experiments we used antisera collected 11 days after the third boost.

Antiserum against the truncated TrpE 37 kDa protein expressed by the pATH3 vector was prepared in a similar fashion, however, the majority of the TrpE protein was found in the soluble fraction. Preimmune serum was collected before the initial injections.

Western blots

Lymantria dispar cells were grown in 75 cm^2 T-flasks and were infected with first passage OpMNPV at a multiplicity of infection (moi) ranging from 5 to 400. Cells were harvested at various times post infection (hours post infection, hpi) and cell lysates at a concentration of $4x10^6$ cells/ml were prepared as described by Quant-Russell et al., 1987). PMSF (0.5 mM) was added to the cells while harvesting and to the lysates in order to inhibit protease degradation of susceptible proteins. Samples for Western blot analysis were electrophoresed on 9 or 12% SDS polyacrylamide gels (Laemmli, 1970). Proteins from the gels were electroblotted onto nitrocellulose membranes and an ELISA was performed on the immunoblots as described previously (Quant-Russell et al., 1987). Anti-TrpE-p32 antiserum was used on the Western blots at a dilution of 1:250 in TBS-Tween (20 mM Tris, pH 7.5, 500 mM NaCl, 0.05% Tween 20). Controls using rabbit preimmune serum and anti-TrpE antiserum in place of anti-TrpE-p32 antiserum were also performed. No differences in the time course of p32 expression were noted using

different moi.

Immunofluorescent microscopy

Immunoflourescent microscopy studies of OpMNPV infected *L. dispar* cells were performed in a similar manner as described previously (Pearson et al., in press). In order to ensure polyhedra production high moi (up to 600) were used (McClintock et al., 1986). *L. dispar* cells were grown on coverslips until nearly confluent and were infected with first passage OpMNPV. The infected cells were harvested at various times post infection by removing the coverslips from the dishes, rinsing the attached cells in PBS (pH 7.4, Sigma) and fixing in methanol at -20°C for 10 min. The cells were air dried and stored dessicated at -20°C until used. The fixed cells were rehydrated in buffer A (1X PBS pH 7.4, 5% fetal bovine serum, and 0.1% saponin) for 5 to 10 min and immunofluorescent antibody staining was performed as described previously (Pearson et al., in press). The anti-TrpE-p32 antiserum was used at a dilution of 1:16,000 in buffer A and the goat anti-rabbit IgG conjugated with fluorescein isothiocyanate (GAR-FITC, Sigma) was diluted 1:60. Fluorescein stained cells were viewed with a Zeiss epifluorescence microscope using Zeiss excitation filters KP490 and KP500 and barrier filter LP528. Uninfected *L. dispar* cells were treated in the same manner as infected cells. The controls using anti-TrpE rabbit antiserum (diluted 1:16,000) and preimmune serum (diluted 1:16,000) were performed similarly. Fixation of OpMNPV-infected *L. dispar* cells in 10% formaldehyde for 10-15 min at RT followed by three 6-10 min washes in buffer A was also performed.

Immunofluorescent microscopy studies on polyhedra were performed as described by Whitt and Manning (1988). A 3 μl volume of OpMNPV polyhedra at 5 mg/ml was spread on a glass slide and air dried for at least 10 min. The polyhedra were dissociated on the slide by incubation at RT in 100-150 μl dilute alkaline saline (DAS; 50 mM Na_2CO_3, 50 mM NaCl) for 5 min. The slides were repeatedly immersed in PBS (pH 7.4, Sigma) in order to stop dissociation and

remove solubilized protein. Immunofluorescent staining was carried out as described previousy (Whitt and Manning, 1988) with anti-TrpE-p32 rabbit antiserum diluted 1:16,000 in buffer A and a 1:60 dilution of GAR-FITC (Sigma). The polyhedra were viewed under a Zeiss microscope as described above using a 100X oil immersion objective. Controls using anti-TrpE rabbit antiserum (diluted 1:16000), preimmune serum (diluted 1:16,000), and a monoclonal antibody (MAb) to polyhedrin (Quant, et al., 1984) (diluted 1:1000) were performed.

Cells and polyhedra were photographed with T-max 400 film (Kodak) using a 45 second exposure time for immunofluorescence and a two second exposure time for phase-contrast.

RESULTS

Localization and nucleotide sequencing of the p32 gene

Polyclonal mouse antiserum produced against purified OpMNPV polyhedra-derived virion proteins was used to screen a lambda gtll expression library of OpMNPV DNA. A number of immunoreactive clones were selected and screened with a monoclonal antibody to p10, monoclonal antibodies to p39 (Pearson et al., in press) and polyclonal rabbit antiserum to polyhedrin (PH) in order to eliminate clones containing DNA inserts from these previously studied genes. Insert DNA from two lambda gtll recombinants (L2 and L4) immunoreactive with PDV polyclonal antisera, but nonreactive to p10, p39 or polyhedrin antisera, hybridized to the HindIII-M fragment on Southern blots of OpMNPV cosmid and genomic DNA (Fig. 1). Insert DNA from clones L2 and L4 was subcloned into M13 and sequenced. This region was also sequenced using subcloned restriction enzyme fragments and exonuclease III deletion mutants of HindIII-M DNA (Fig. 2). An open reading frame (ORF) encoding a protein of 32 KDa was identified (Fig. 2). The L2 and L4 inserts were located at different, nonoverlapping regions within this ORF (Fig. 2). Double-stranded lambda DNA sequencing of the L2 clone indicated that its insert was oriented in the direction of the ORF. The p32 gene is the third of five ORFs (Gombart et al., in preparation) in the HindIII E-M region and is found upstream of the p26 (Bicknell et al., 1987), p10 and p74 genes (Leisy et al., 1986) (Fig. 1). Analysis of the 5′ flanking nucleotide sequence of the p32 gene revealed the presence of the 14-mer GAGATAAGTTATTA with the conserved ATAAG core which has been found associated with the mRNA start site of all late expressed baculovirus genes that have been characterized thus far (Rohrmann, 1986). Although the significance of this sequence is not known, it has been suggested that it is important in specifying the initiation and/or affecting the levels of transcription of late mRNAs (Rohrmann, 1986). The translational start (ATG) for the p32 ORF follows Kozak's rules for efficient

translation as indicated by the presence of an adenine in the -3 position (Kozak, 1986). Transcriptional mapping of this gene will be described elsewhere (Gombart et al., in preparation).

Time course of p32 synthesis and comparison to p39 synthesis

In order to investigate the expression of the p32 protein, a gene fusion containing the complete p32 ORF fused to the truncated *trpE* gene of the pATH3 bacterial expression vector (Dieckmann and Tzagoloff, 1985) was constructed (Fig. 3). The TrpE-p32 fusion protein was purified on SDS-PAGE gels and the fusion protein of approximately 70 kDa was used to immunize rabbits. The resulting polyclonal antiserum was used in Western blot and immunofluorescent microscopy studies.

The p32 protein is associated with PDV and not BV as anti-TrpE-p32 antiserum reacted with a polyhedra-derived virus (PDV)-associated protein of 32 kDa (Fig. 4a), but did not react with any budded virus (BV) proteins (Fig. 4a). Staining of the 32 kDa protein was also observed in extracts from OpMNPV-infected *O. pseudotsugata* larvae, but not in uninfected *O. pseudotsugata* larvae (Fig. 4a). Synthesis of p32 was followed both by Western blots of OpMNPV-infected cell lysates electrophoresed on SDS-polyacrylamide gels and by fluorescent antibody staining of OpMNPV-infected *L. dispar* cells. Using the anti-TrpE-p32 antiserum for Western blot analysis, a faint band of approximately 32 kDa was first detected at 24 hpi (Fig. 4b). The 32 kDa protein increased in intensity from 36 hpi through 72 hpi (Fig. 4b). Controls included reaction of anti-p32 antiserum against uninfected *L. dispar* cells (Fig. 4b) and anti-TrpE antiserum and preimmune serum reacted against Western blots of infected cells. A protein of 32 kDa was not detected in these controls (data not shown). To correlate the synthesis of the p32 protein to the p39 protein (Pearson, et al., in press), which is a major structural protein of BV and PDV, SDS-PAGE of OpMNPV infected *L. dispar* cell lysates from various times post infection were electroblotted and stained with a mixture of the anti-p32 antiserum

and a MAb to p39. The p39 MAb strongly stained a 39 kDa band at 24 hpi while p32 appeared as a faintly staining band at 24 hpi (Fig. 4c). Both the p39 and p32 bands increased in intensity as infection progressed with the p39 band staining more strongly than the p32 band at each time point (Fig. 4c).

In immunofluorescent microscopy studies, the p32 protein was not detected at 18 hpi (data not shown), but at 24 hpi a low level of staining in the cytoplasm and nucleus was observed (Fig. 5). Increased staining of the cells was observed at 36 and 48 hpi (Fig. 5) with fluorescence concentrated at the periphery of the cells in the cytoplasm at 48 hpi, thereby creating a bright ring-like appearance. At 60 hpi, the ring-like staining was still present, but with slightly less intensity and an overall even staining of the cell cytoplasm and nucleus was observed (Fig. 5). Examination of 48 and 60 hpi cells with phase-contrast revealed that those fluorescing most brightly also contained numerous polyhedra (Fig. 5). Controls using anti-TrpE antiserum and preimmune serum on uninfected and OpMNPV-infected *L. dispar* cells did not stain similarly to those reacted with anti-TrpE-p32 antiserum (data not shown). Also, anti-TrpE-p32 antiserum was not observed to stain uninfected *L. dispar* cells (data not shown). Immunofluorescence with formaldehyde fixed cells resulted in observations similar to those described above (data not shown).

Immunofluorescent microscopy of polyhedra

To determine the relationship of the p32 protein to components of viral polyhedra, immunofluorescent microscopy of alkali dissolved polyhedra was performed using procedures similar to those recently reported by Whitt and Manning (1988). Incubation with anti-TrpE-p32 antiserum resulted in the staining of the periphery of the polyhedra (Fig. 6a). This ring-like staining of the polyhedra indicates an even distribution of p32 on the polyhedral membrane. Incubation with a MAb to polyhedrin resulted in various degrees of staining of the polyhedra from very faint to

very bright fluorescence with no specific pattern observed (Fig. 6b). When DAS-treated polyhedra were incubated with control antiserum (anti-TrpE antiserum or rabbit preimmune serum) staining of the polyhedra was not observed (data not shown). The data above further suggests that p32 is associated with the polyhedral membrane.

Localization of major components in polyhedra solubilized under different conditions.

In order to further elucidate the relationship of the p32 protein with the polyhedral membrane, dissolution studies with OpMNPV polyhedra were performed similar to that described by Whitt and Manning (1988) (Fig. 7). OpMNPV polyhedra were dissociated in dilute alkaline saline (DAS) and centrifuged at 12,000 x g. The resulting pellet was incubated with SDS or SDS plus 2-mercaptoethanol (Fig. 7). Western blot analysis was carried out with antibodies to three different proteins (anti-p32 antiserum; a MAb to p39 (Pearson et al., in press), and a MAb to polyhedrin (Quant et al., 1984)). Through Western blot analysis, it was demonstrated that incubation of polyhedra with DAS resulted in the solubilization of polyhedrin as evidenced by its presence in the supernatant fraction with only trace amounts in the pellet and subsequent fractions (Fig. 7, panel A). In contrast, Western blot analysis of the DAS-treated polyhedra using the MAb to p39 (a major viral structural protein) and anti-p32 antiserum revealed these proteins were found predominantly in the DAS pellet fraction (Fig. 7, panels B and C). In Western blot analysis of the SDS treated DAS pellet fraction, it was demonstrated that p39 was solubilized and the majority found in the supernatant as expected for a virion protein (Fig. 7, panel B). However, the majority of the p32 protein was found in the pellet indicating it was not solubilized by SDS (Fig. 7, panel C). Treatment of the DAS pellet fraction with both SDS and 2-mercaptoethanol resulted in the solubilization of p39 (Fig. 7, panel B) and p32 (Fig. 7, panel C) as evidenced by the

majority of both proteins present in the supernatant fraction. The solubilization of the p32 protein upon treatment with a reducing agent indicates that p32 may be associated via a thiol linkage through cysteine residues with the polyhedral envelope.

On each blot in Fig. 7, control lanes containing polyhedrin (PH), purified TrpE-p32 fusion protein (F32), and polyhedra-derived virus proteins (PDV) were included. The MAb to polyhedrin stained polyhedrin protein in lanes PH and PDV, but not the purified TrpE-p32 fusion protein (Fig. 7, panel A) indicating that the p32 protein which is very similar in size to polyhedrin is not an altered form of polyhedrin. The p39 MAb reacted only with a 39 kDa protein in the PDV lane (Fig. 7, panel B). Anti-TrpE-p32 antiserum did not react with polyhedrin, but did react with a 32 kDa protein in the PDV and the TrpE-p32 fusion protein of 70 kDa (Fig. 7, panel C) providing further evidence that this antiserum reacts with an immunologically different protein similar in size to polyhedrin.

Through reciprocal Western blot analysis, it was found that the anti-TrpE-p32 antiserum cross reacted with an approximately 34 kDa protein of dissolved AcMNPV PDV and a monoclonal antibody to the pp34 protein of AcMNPV was found to cross react with a 32 kDa protein of dissolved OpMNPV PDV (data not shown).

Relatedness of OpMNPV p32 gene and AcMNPV pp34 gene

To locate the gene in the AcMNPV genome homologous to the OpMNPV p32 gene, insert DNA from the OpMNPV lambda gt11 recombinant, L2 (Fig. 2), was hybridized under non-stringent conditions (30% formamide) to Southern blots of AcMNPV genomic DNA (Maniatis, et al., 1982). The OpMNPV DNA hybridized to the HindIII-A and XhoI-I fragments of AcMNPV (data not shown). The genomes of OpMNPV and AcMNPV have been shown to be colinearly organized (Leisy et al., 1984) and the position of hybridization to the AcMNPV pp34 gene indicates that the genes for this polyhedral envelope-associated protein are present in similar regions of the genomes. The sequence of approximately 5 kbp of this region in AcMNPV was recently

reported and five ORFs were identified and transcriptionally mapped (Oellig et al., 1987). Comparison of the OpMNPV p32 predicted amino acid sequence with that of the AcMNPV ORF 3 (Oellig et al., 1987) revealed a 58% amino acid identity between the OpMNPV and AcMNPV proteins (Fig. 8). The AcMNPV ORF 3 gene which encodes a predicted protein of 36 kDa is unusual in that it contains 16 arginine-serine repeats (starting at amino acid 101) which are not found in the OpMNPV p32 predicted protein (Fig. 8). A proline rich sequence (PCPQP) is repeated twice in the OpMNPV amino acid sequence (starting at amino acid 112) and in the same region in AcMNPV (starting at amino acid 115) a proline rich sequence (PHCRP) is also found to be repeated twice (Fig. 8). In the OpMNPV amino acid sequence, a proline and serine rich sequence (PPSCS, starting at amino acid 58) is found repeated twice with one amino acid residue difference in the second repeat (PPSNS, starting at amino acid 64). The effect of the insertion of these repeats in the two proteins on predicted hydropathy plots of each protein was determined (Fig. 9). The location and size of each insertion is denoted by a solid bold line on the hydropathy plot. It appears that the proteins share many regions of similarity (Fig. 9). The insertion of the PPSCS/PPSNS repeat in the OpMNPV p32 protein, however, introduces a region of hydrophilicity as does the insertion of the 16 arginine-serine repeats in the ORF 3 protein of AcMNPV (Fig. 9). Cysteine residues, which may be involved in the thiol linkage of the protein with the carbohydrate of the polyhedral envelope, are clustered primarily in the hydrophilic areas of the N-terminal region of both proteins (Fig. 9).

DISCUSSION

In this report, we used a polyclonal antiserum against purified PDV virions to screen a lambda gtll library and isolated a gene encoding a 32 kDa protein. Using polyclonal antibodies made against a TrpE-p32 fusion protein containing the entire protein, we demonstrated that it is expressed late in infection and appears to be associated with the polyhedral envelope of OpMNPV. The predicted amino acid sequence from the OpMNPV p32 gene was found to share a high degree of homology with the third open reading frame (ORF 3) of five reported by Oellig et al. (1987).

Western blot analysis indicated that p32 is associated with the PDV and not the BV phenotype (Fig. 4a). This would be expected for a protein associated with the polyhedral envelope since this envelope is found surrounding the crystalline matrix of mature polyhedra formed late in infection. Comparison of p39, a major structural protein of the PDV, synthesis (Pearson et al., in press) and p32 synthesis by Western blot analysis indicates that both p39 and p32 are detected late in infection with the p39 band staining more intensely at each time point post infection (Fig. 4c). The relatively low intensity of staining of the p32 band on Western blots suggests that p32 may be sythesized at a lower rate than p39 during infection, however, differences in staining intensity between the two protein bands due to properties of the antisera have not been ruled out. The pattern of staining observed in immunofluorescent microscopy studies for p32 differs from that of p39 (Pearson et al., in press) as well. The protein p39 is first evident in the cytoplasm at 24 hpi and accumulates in the nucleus at 36-48 hpi. Beyond 48 hpi, intense nuclear staining with little or no cytoplasmic staining is observed. In contrast, p32 appears in the cytoplasm and nucleus at 24 hpi through 60 hpi with an increasing intensity of staining in the periphery (cytoplasm) of the cells. The increased concentration of fluorescence at the periphery of the cells stained with anti-TrpE-p32 antiserum may be due to several factors. The continuous production of p32 with a low rate

of transport into the nucleus or the swelling of the nucleus causing a decrease in the volume of the cytoplasm (thereby concentrating its contents) or a combination of both may be responsible. The polyhedral envelope which surrounds the mature polyhedra is probably the last component added in the maturation process. Therefore, it is likely that synthesis of the p32 protein may not be regulated in the same manner as the synthesis of some other proteins required earlier in the development of polyhedra-derived virus.

Results from Western blot analysis of DAS-dissociated polyhedra indicated that treatment of the DAS-P fraction (which contains virions and the polyhedral envelope) with SDS resulted in the solubilization of virion proteins. The p32 protein, however, remained insoluble and was solubilized only upon treatment with SDS and a reducing agent (2-mercaptoethanol), suggesting that it may be covalently attached to the polyhedral envelope via a thiol-glycosidic linkage. Linkages of this type have been observed for erythrocyte membrane glycopeptides (Weiss, et al., 1971) and a glycopeptide isolated from human urine (Lote and Weiss, 1971). Further evidence for the association of p32 with the envelope came from immunofluorescent microscopy studies on DAS dissociated polyhedra. The distinct staining of the periphery of the polyhedra with the anti-TrpE-p32 antiserum indicates that the p32 is found evenly distributed around the polyhedral envelope (Fig. 6a) and suggests that the OpMNPV p32 protein is associated with polyhedra and does not appear to be a structural protein of the virion. This result is similar to that demonstrated by Whitt and Manning (1988) for the AcMNPV polyhedral envelope-associated phosphoprotein pp34.

The comparison between the predicted amino acid sequences of the OpMNPV p32 gene and ORF 3 at 82.8 map units in AcMNPV revealed a high degree of amino acid identity (Fig. 8). Comparison of the hydropathy plots of these two proteins (Fig. 9) indicates that the AcMNPV arginine-serine repeats contribute to an extremely hydrophilic region in the protein. The OpMNPV proline-serine rich repeats are also a component of a hydrophilic region. It is

possible that the very large hydrophilic region created by the 16 arginine-serine repeats in the AcMNPV ORF 3 protein may have a significant effect on the structure of this protein. The presence of a cluster of cysteine residues in each protein in a hydrophilic area (amino acid residues 107, 113, 118 and 125 in OpMNPV and amino acid residues 94, 117 and 126 in AcMNPV) (see Figs. 8 and 9) may be important in the thiol linkage of these proteins to the polyhedral envelope. The repeated sequence in the AcMNPV gene may make the cysteines more available for linkage to the carbohydrate of the polyhedral envelope. The repeat PCPQP in the OpMNPV sequence is similar to one (PHCRP) in a homologous region of the AcMNPV amino acid sequence (Fig. 8). The presence of this proline-rich repeat in both proteins suggests it may play an important role in the structure and function of these proteins.

Our investigation suggests that the gene encoding the OpMNPV p32 protein is the homolog to ORF 3 reported by Oellig et al. which encodes the polyhedral envelope-associated protein of AcMNPV. Both the OpMNPV p32 protein and the pp34 protein of Whitt and Manning (1988) appear to be associated with the polyhedral envelope via thiol linkages. Additionally, our anti-TrpE-p32 antiserum reacted with a protein of about 34 kDa on immunoblots of dissolved AcMNPV polyhedra and a MAb to AcMNPV pp34 reacted with a protein of 32 kDa on immunoblots of dissolved OpMNPV polyhedra (data not shown). Therefore, we conclude that ORF 3 of AcMNPV encodes the polyhedral envelope-associated phosphoprotein, pp34, which is homologous to the 32 kDa polyhedral envelope-associated protein of OpMNPV.

Figure II. 1. A) HindIII restriction enzyme map of the OpMNPV genome indicating the location of the genes for the structural proteins polyhedrin (PH) and p39. B) Enlargement of the HindIII M-Q region of the OpMNPV genome showing the location of the lambda gtll fusions 2 and 4 (L2 and L4, respectively) in the gene for the protein p32 (ORF 3). The locations of ORFs 1-5 and the genes for p26, p10 and p74 are indicated. Abbreviations: Bg, BglII; C, ClaI; H, HindIII; K, KpnI; P, PstI; S, SalI; Ss, SstI; X, XhoI.

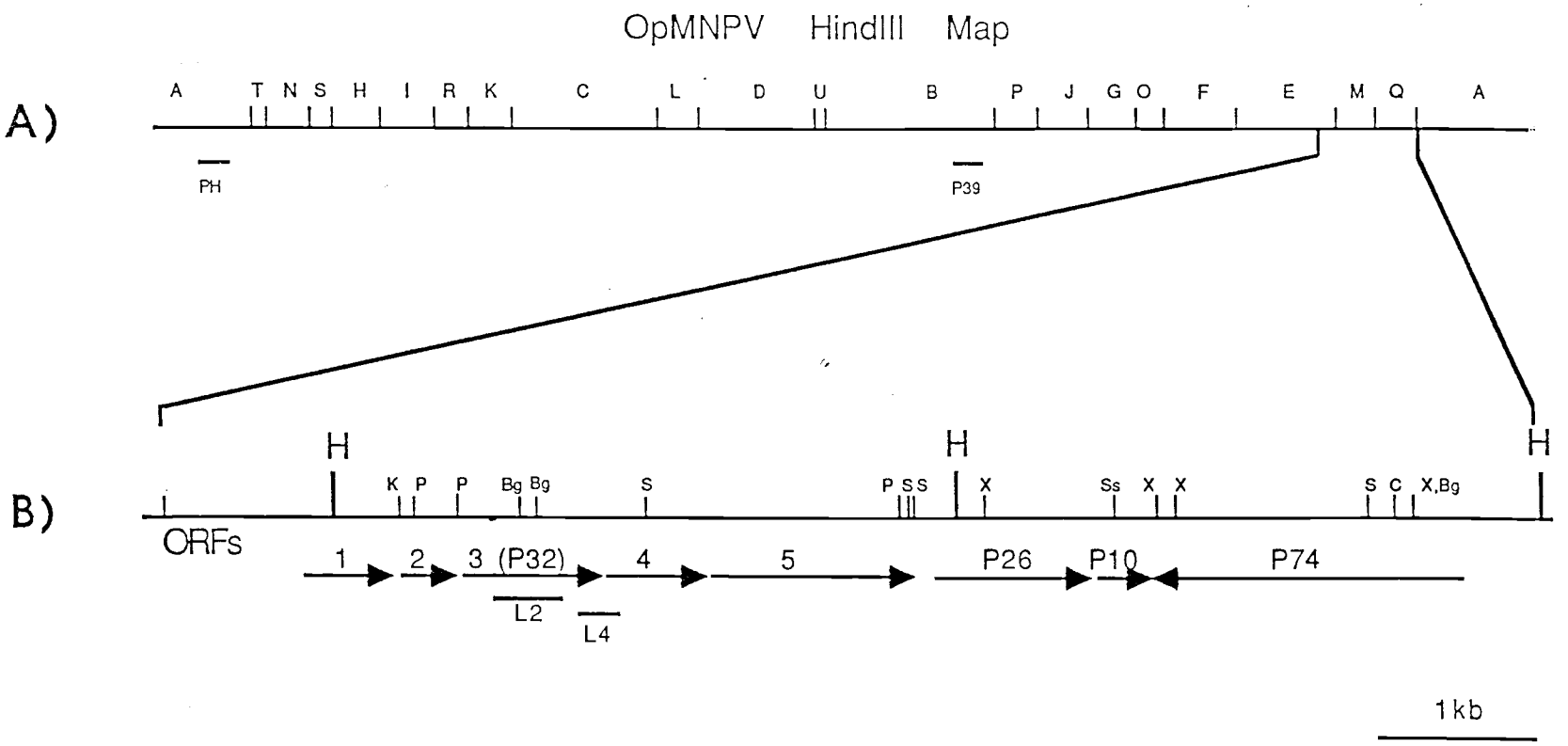
OpMNPV HindIII Map
A)
A T N S H I R K C L D U B P J G O F E M Q A
PH
P39
B)
H H H
K P P Bg Bg S P S S X Ss X X S C X,Bg
ORFs
1 2 3 (P32) 4 5 P26 P10 P74
L2
L4
1kb

Figure II.1

Figure II. 2. Nucleotide and predicted amino acid sequences of the polyhedral envelope protein gene (p32) of OpMNPV. The positions of two immunoreactive lambda gtll fusions (L2 and L4) are indicated at nucleotide (nt) 266 and nt 760 respectively. The position of the TrpE fusion produced by partially deleting the 5' flanking region and fusing the ORF in frame with the truncated *trpE* gene of the pATH3 expression vector is indicated at nt 79. The conserved 14-mer found upstream of baculovirus late genes is underlined. The proline-rich repeat PCPQP (starting at amino acid 112) and the proline/serine rich repeats PPSCS and PPSNS (starting at amino acids 58 and 64, respectively) are underlined. The predicted amino acid sequence is given below the corresponding codons.

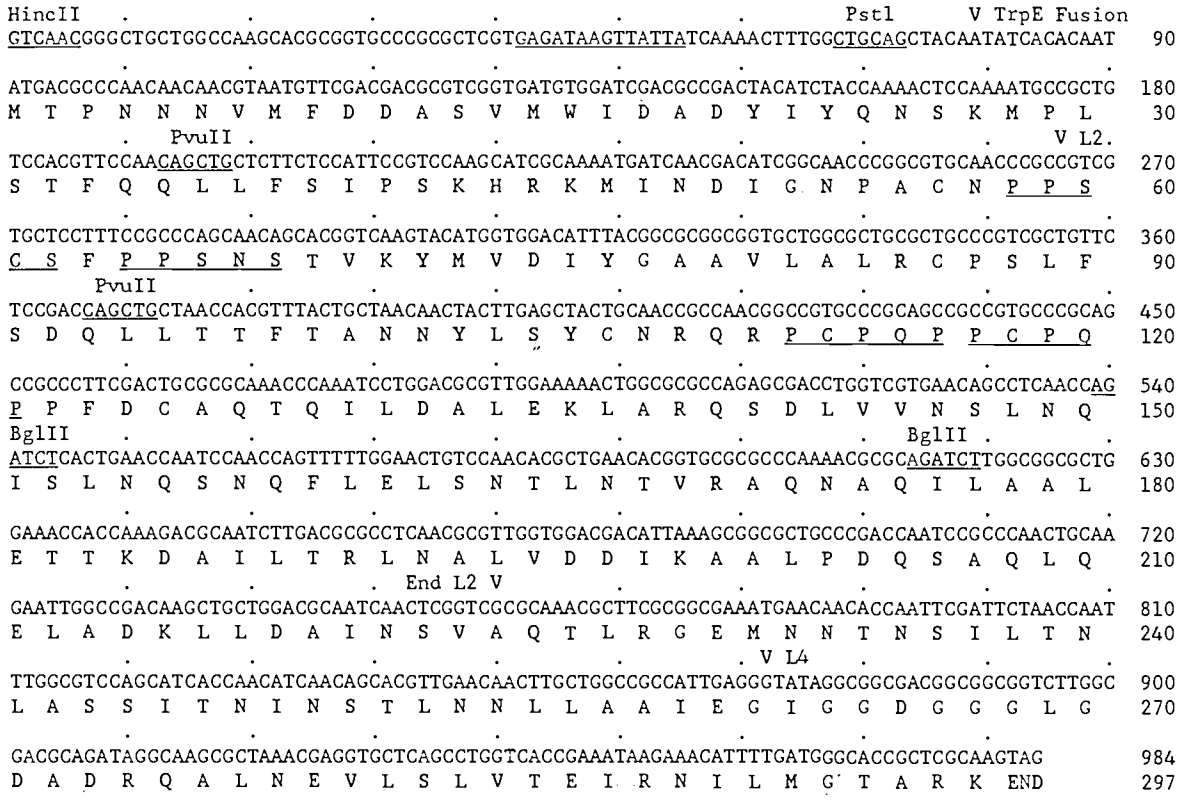
HincII
PstI
V TrpE Fusion
PvuII
V L2.
PvuII
BglII
BglII
End L2 V
V L4

Figure II.2

Figure II. 3. Construction of the *trpE*-p32 gene fusion. A) Restriction map of HindIII-M region showing the position of the p32 gene (ORF 3) relative to the other four ORFs. The position of the two lambda clones L2 and L4 from the p32 gene are indicated. B) Organization of the *trpE*-p32 gene fusion. The entire p32 gene (predicted protein MW of 32.4 kDa) was ligated to the truncated *trpE* gene (protein MW of 37 kDa) which resulted in a fusion protein with a MW of approximately 70 kDa. The translational start codon (ATG) and the termination codon (TAG) of the p32 ORF are indicated. C) Nucleotide sequence of the *trpE*-p32 gene fusion junction. The construction of this plasmid is described in the Materials and Methods. Twelve extra nucleotides from sequence upstream of the translational start site (ATG) of p32 and 18 nt from the M13mp18 polylinker region are present in the fusion. Abbreviations: Same as in Fig.1 legend.

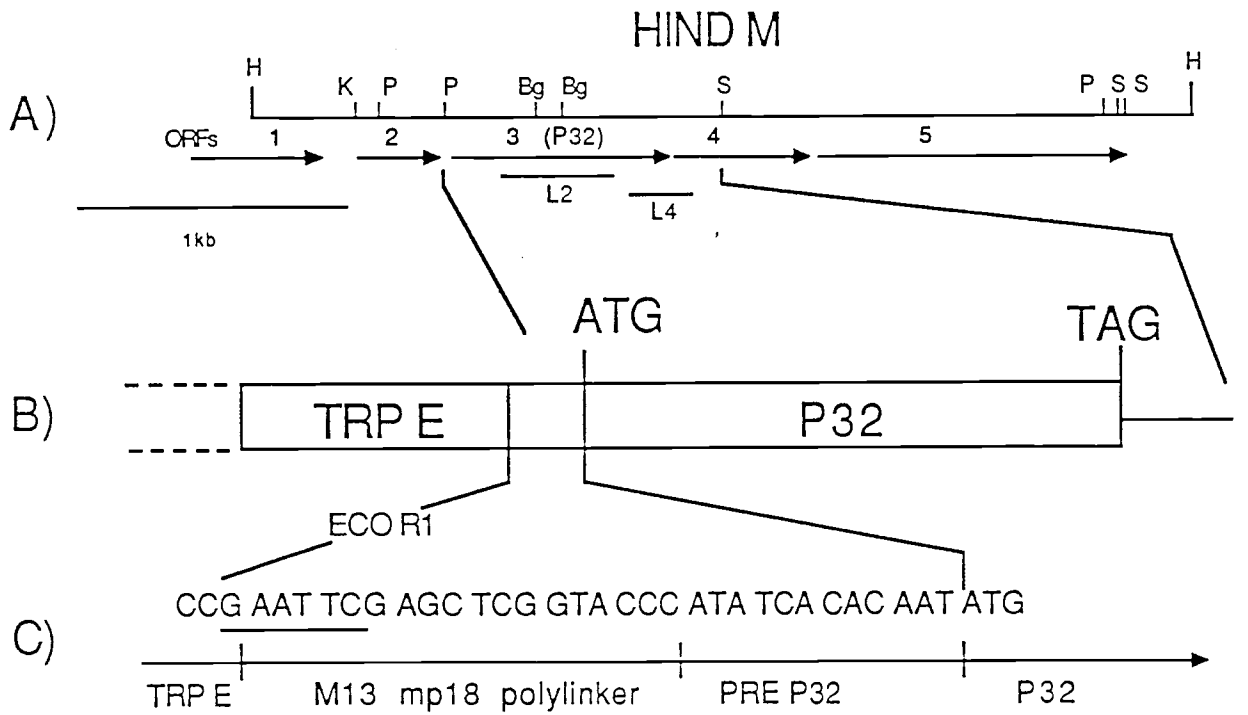
HIND M
A)
H
K
P
P
Bg
Bg
S
P
S
S
H
ORFs
1
2
3
(P32)
4
5
L2
L4
1kb
ATG
TAG
B)
TRP E
P32
ECO R1
CCG AAT TCG AGC TCG GTA CCC ATA TCA CAC AAT ATG
C)
TRP E
M13 mp18 polylinker
PRE P32
P32

Figure II.3

Figure II. 4. Western blot analysis of the p32 protein in OpMNPV virions and in OpMNPV infected *L. dispar* cells. A) Western blot (electrophoresed on 12% SDS-polyacrylamide gel) of structural proteins from PDV and BV virions and extracts from uninfected (U) and OpMNPV-infected (I) *O. pseudotsugata* larvae using the anti-p32 antiserum. B) Western blot (electrophoresed on 12% SDS-polyacrylamide gel) of infected cell extracts at various times post infection (pi) using the anti-p32 antiserum. C) Western blot (electrophoresed on 9% SDS-polyacrylamide gel) of infected cell extracts at various times pi using a mixture of both the anti-p32 antiserum (1:250 dilution) and undiluted tissue culture fluid of a p39 monoclonal antibody (MAb 236) (Pearson et al., in press). The numbers at the top of each well indicate the hours post infection. Cell lysates were boiled in sample buffer for 2-3 min and 12 μl (equivalent to 4.8×10^4 cells) was loaded per lane and about 2 μg of purified OpMNPV PDV and BV structural proteins were loaded per lane. The numbers at the right of the figures indicate the size in kDa of the immunoreactive proteins. The numbers at the left indicate the positions of the protein markers. Abbreviations: PDV, polyhedra derived virus; BV, budded virus; U, uninfected insect larvae; I, OpMNPV infected insect larvae 8 days post infection (Quant et al., 1984).

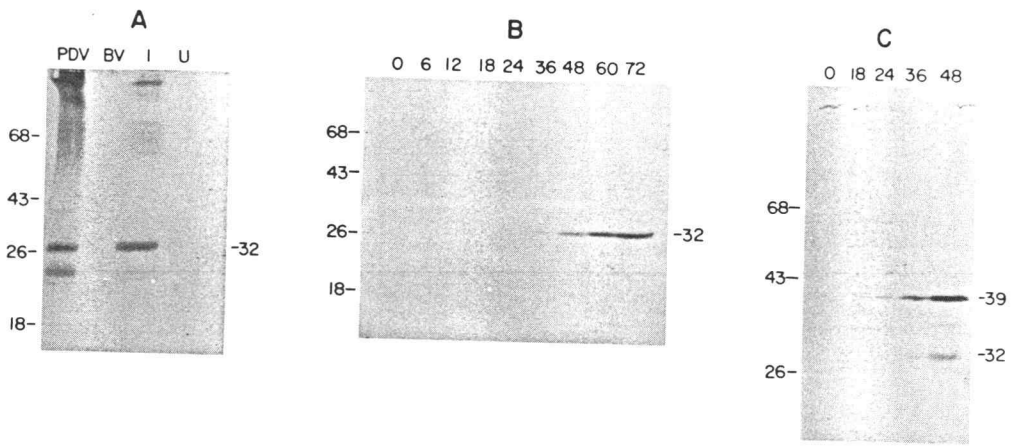
A
PDV BV I U
68-
43-
26-
18-
-32
B
0 6 12 18 24 36 48 60 72
68-
43-
26-
18-
-32
C
0 18 24 36 48
68-
43-
26-
-39
-32

Figure II.4

Figure II. 5. Fluorescent staining of methanol fixed OpMNPV-infected *L. dispar* cells with anti-TrpE-p32 antiserum (diluted 1:16,000). Micrographs of fluorescein stained cells are at the left and the hpi is denoted by a number in the lower left corner of the micrograph. The corresponding phase-contrast micrographs are at the right and the hpi in the lower left corner are denoted with a prime (′). Micrographs were taken at 400X magnification. The bar indicates 10 μm.

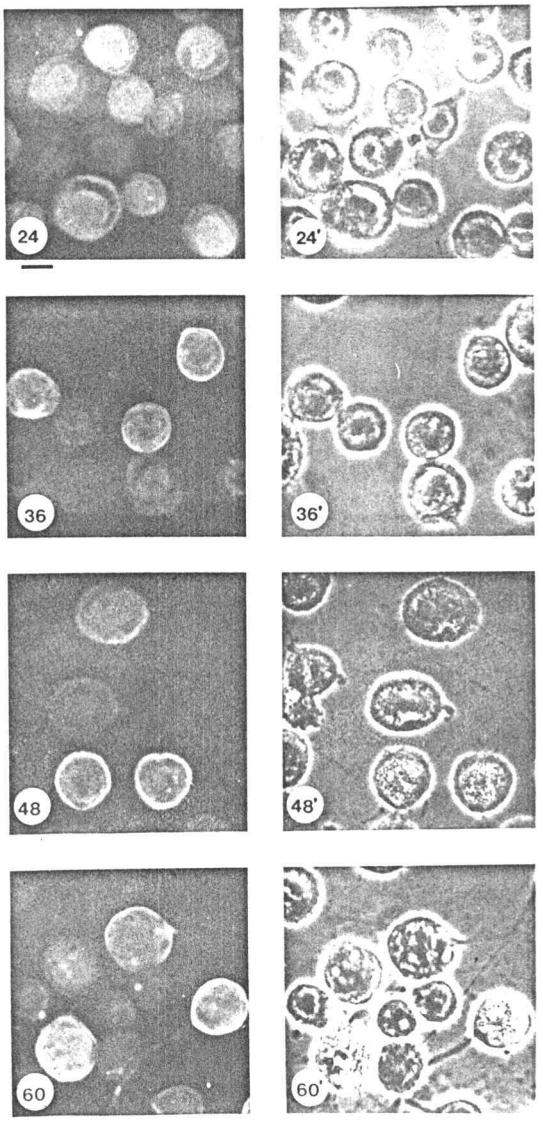

Figure II.5

Figure II. 6. Fluorescent staining of alkali dissolved OpMNPV polyhedra. A) Fluorescent staining of polyhedra with anti-TrpE-p32 antiserum. B) Fluorescent staining of polyhedra with anti-polyhedrin monoclonal antibody (Quant, et al., 1984). Treatment of the polyhedra for immunofluorescent staining is described in the Materials and Methods. Micrographs were taken at 1000X with oil immersion. The bar indicates 5 μm.

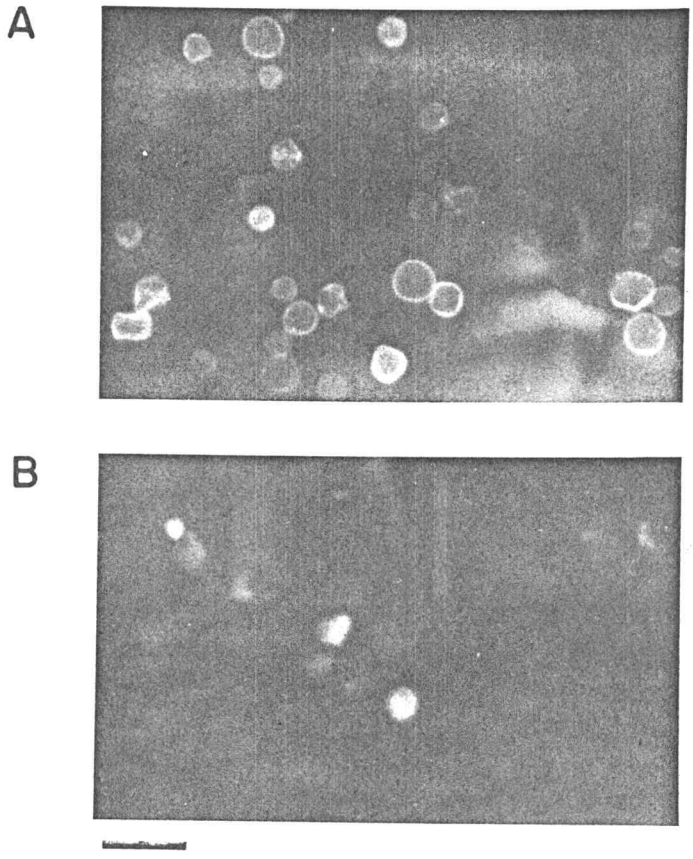

Figure II.6

Figure II. 7. Western blot analysis to localize major viral structural proteins in polyhedra solubilized under different conditions. Three similarly prepared Western blots are shown and were reacted with the following: A) Anti-polyhedrin (AS-PH) monoclonal antibody (1:800 dilution) (Quant et al., 1984); B) Anti-p39 (AS-P39) monoclonal antibody (MAb 236) (undiluted tissue culture supernatant) (Pearson et al., submitted); C) Anti-TrpE-p32 (AS-P32) antiserum (1:250 dilution). The numbers on the right indicate the size of the major immunoreactive bands. The numbers at the left indicate the positions of the protein markers. The dissolution protocol was similar to that described by Whitt and Manning (1988) except it was found that heating the sample at 60°C for 5 min resulted in more complete dissolution. OpMNPV polyhedra (about 1 mg) were incubated at 70°C for 20 min to inactivate protease activity, then incubated with an equal volume of dilute alkaline saline (DAS; 50 mM Na_2CO_3, 50 mM NaCl) at 60°C for 5 min, cooled on ice for 1-2 min and centrifuged at 12,000 x g for 10 min at 4°C. The supernatant (DAS-S) was removed and the pellet (DAS-P) was resuspended in 150 μl of 10 mM Tris (pH 7.5) and divided into three 50 μl fractions. One fraction of DAS-P was untreated. The second fraction of DAS-P (SDS) was incubated with 0.5% SDS at 60°C for 5 min, cooled to room temperature and centrifuged at 12,000 x g for 10 min. The supernatant (SDS-S) was removed and the pellet (SDS-P) was resuspended in 50 μl of 10 mM Tris (pH 7.5). The third fraction of DAS-P (2ME/SDS) was incubated in 0.5% SDS and 1% 2-mercaptoethanol at 60°C for 5 min, cooled to room temperature and centrifuged at 12,000 x g for 10 min. The supernatant (2ME/SDS-S) was removed and the pellet (2ME/SDS-P) was resuspended in 50 μl of 10 mM Tris (pH 7.5). Each of the supernatants were brought up to 50 μl volume with 10 mM Tris (pH 7.5). Each sample was mixed with an equal volume of 2X reducing sample buffer, boiled for 3-5 min and electrophoresed through a 9% SDS-polyacrylamide gel (AS-PH blot, 12% SDS-polyacrylamide gel), transferred to a nitrocellulose membrane and immunoblotted as described under Methods and Materials. Controls include polyhedrin (PH), gel purified TrpE-p32 fusion (F32) and

purified structural proteins of the polyhera-derived virus (PDV). The following amounts were loaded: A) 1 μl of resuspended pellets and supernatants; PH, 0.6 μg; F32, 0.4 μg; PDV, 2 μg. B) 10 μl of resuspended pellets and supernatants; PH, 3.8 μg; F32, 0.4 μg; PDV, 2 μg. C) 10 μl of resuspended pellets and supernatants; PH, 0.6 μg; F32, 0.4 μg; PDV, 2 μg.

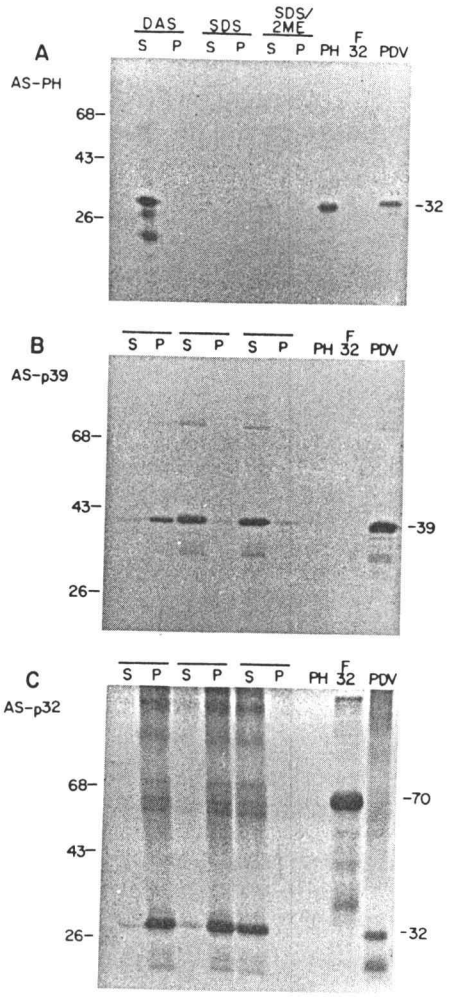
DAS
SDS
SDS/
2ME
S P S P S P PH F 32 PDV
A
AS-PH
68-
43-
26-
-32
B
AS-p39
-39
C
AS-p32
-70

Figure II.7

Figure II. 8. Comparison of the predicted amino acid sequences from the OpMNPV p32 gene and the AcMNPV ORF 3 gene (Oellig et al., 1987). The dots indicate identical amino acids. 58% identity in amino acid sequence is observed between the two proteins. The 16 arginine-serine repeats (starting at amino acid 101) in AcMNPV are underlined. The two PHCRP repeats (starting at amino acid 115) in the AcMNPV sequence, the two PCPQP repeats (starting at amino acid 112) and the PPSCS/PPSNS repeat (starting at amino acid 58) in the OpMNPV sequence are also underlined. The MW of each predicted protein is indicated at the end of each amino acid sequence. A base (C) was inserted at nucleotide 2324 in the AcMNPV sequence in order to arrive at the predicted amino acid sequence given above (Cornelia Oellig, personal communication).

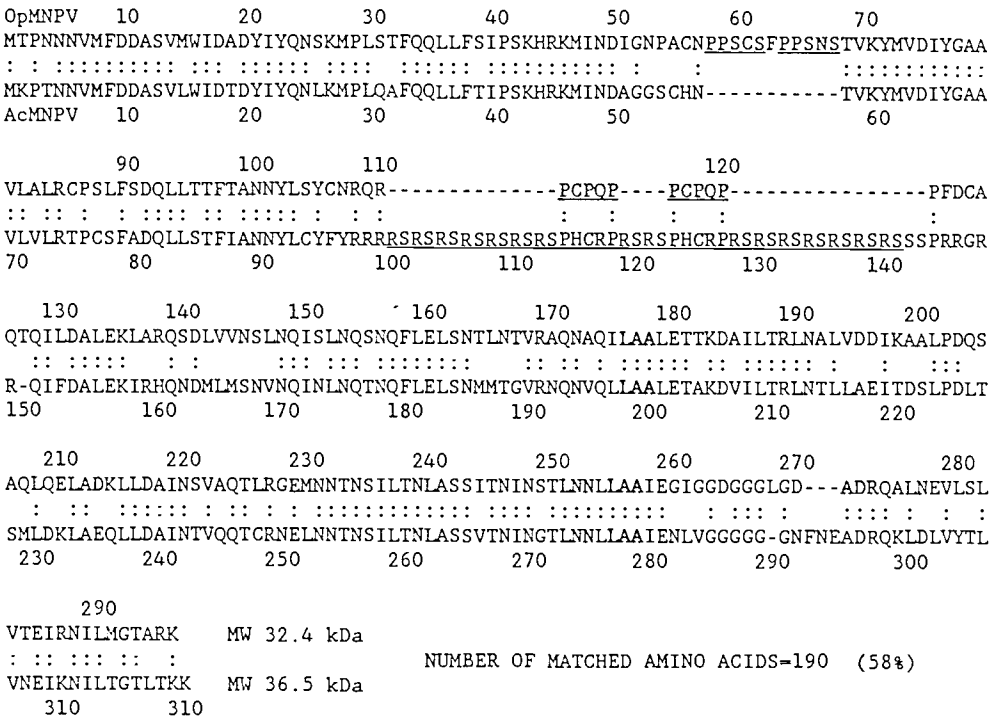
OpMNPV 10 20 30 40 50 60 70
MTPNNNVMFDDASVMWIDADYIYQNSKMPLSTFQQLLFSIPSKHRKMINDIGNPACNPPSCSFPPSNSTVKYMVDIYGAA
MKPTNNVMFDDASVLWIDTDYIYQNLKMPLQAFQQLLFTIPSKHRKMINDAGGSCHN----------TVKYMVDIYGAA
AcMNPV 10 20 30 40 50 60
90 100 110 120
VLALRCPSLFSDQLLTTFTANNYLSYCNRQR----------PCPQP----PCPQP----------PFDCA
VLVLRTPCSFADQLLSTFIANNYLCYFYRRRRSRSRSRSRSRSRSPHCRPRSRSPHCRPRSRSRSRSRSRSSSPRRGR
70 80 90 100 110 120 130 140
130 140 150 160 170 180 190 200
QTQILDALEKLARQSDLVVNSLNQISLNQSNQFLELSNTLNTVRAQNAQILAALETTKDAILTRLNALVDDIKAALPDQS
R-QIFDALEKIRHQNDMLMSNVNQINLNQTNQFLELSNMMTGVRNQNVQLLAALETAKDVILTRLNTLLAEITDSLPDLT
150 160 170 180 190 200 210 220
210 220 230 240 250 260 270 280
AQLQELADKLLDAINSVAQTLRGEMNNTNSILTNLASSITNINSTLNNLLAAIEGIGGDGGGLGD---ADRQALNEVLSL
SMLDKLAEQLLDAINTVQQTCRNELNNTNSILTNLASSVTNINGTLNNLLAAIENLVGGGGG-GNFNEADRQKLDLVYTL
230 240 250 260 270 280 290 300
290
VTEIRNILMGTARK MW 32.4 kDa
NUMBER OF MATCHED AMINO ACIDS=190 (58%)
VNEIKNILTGTLTKK MW 36.5 kDa
310 310

Figure II.8

Figure II. 9. Hydropathy plots of OpMNPV p32 and AcMNPV pp34 proteins. Plots were constructed using the algorithms of Kyte and Doolittle (1982) with an open window of 19 amino acid residues. Top panel: analysis of OpMNPV. The region containing the PPSCS/PPSNS repeat (amino acids 57-68) is indicated by a bold line. In the homologous region of the AcMNPV protein, this repeat is absent. Bottom panel: analysis of AcMNPV. The region containing the 16 arginine-serine repeats (amino acids 101-142) is indicated by a bold line. In the homologous region of the OpMNPV protein, the repeat is absent. The cysteine residues of each protein are indicated by an asterisk (*). Points lying above the solid line indicate sectors with an overall hydrophobic character, whereas points below the solid line indicate sectors with an overall hydrophilic character.

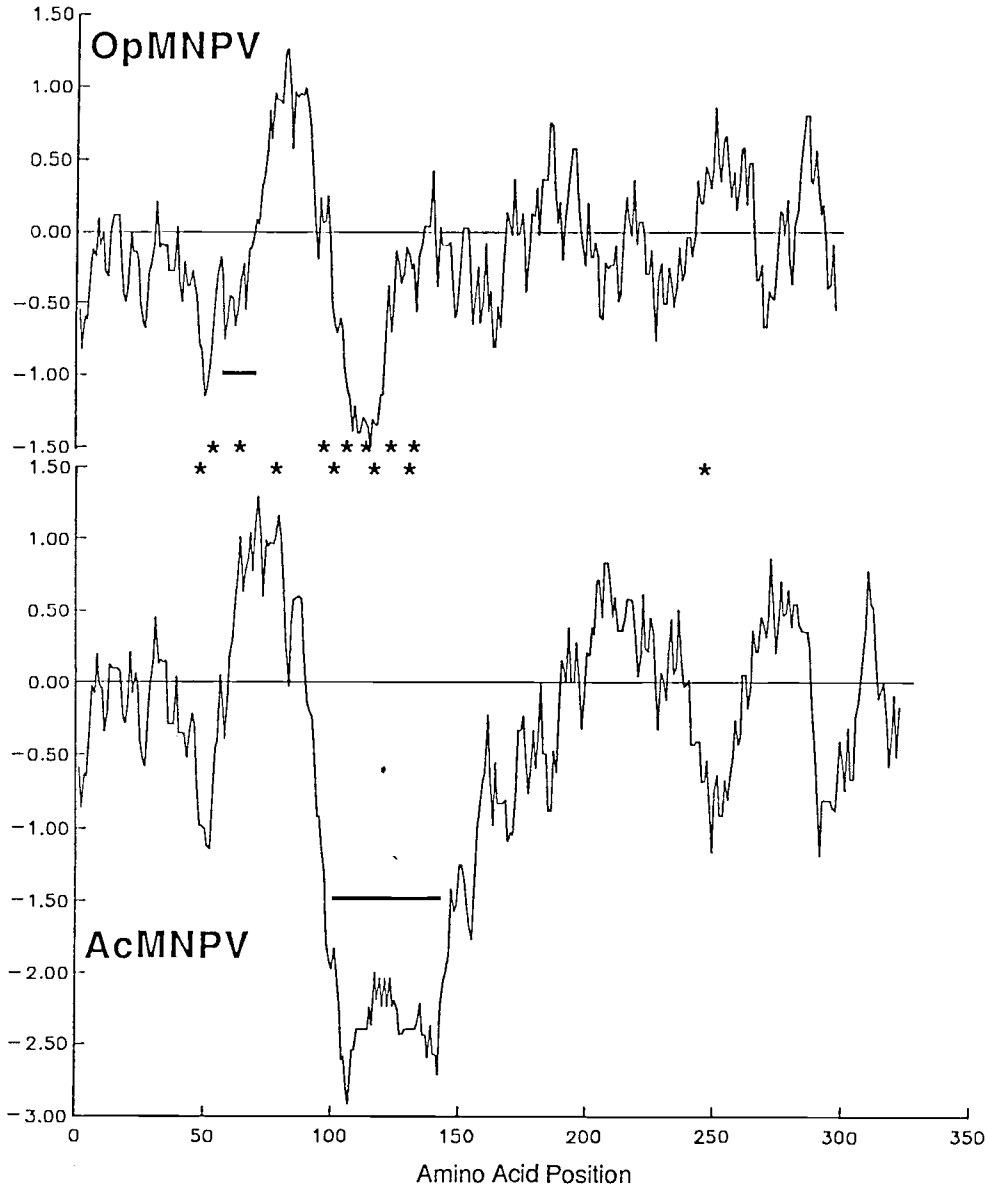
OpMNPV
AcMNPV
1.50
1.00
0.50
0.00
-0.50
-1.00
-1.50
-2.00
-2.50
-3.00
0
50
100
150
200
250
300
350
Amino Acid Position

Figure II.9

REFERENCES

Bicknell, J.N., Leisy, D.J., Rohrmann, G.F., and Beaudreau, G.S. (1988). Comparison of the p26 gene region of two baculoviruses. Virology 161 , 589-592.

Dieckmann, C.L. and Tzagoloff, A. (1985). Assembly of the mitochondrial membrane system. Journal of Biological Chemistry 260, 1513-1520.

Feinberg, A.P. and Vogelstein, B. (1984). A technique for radiolabelling DNA restriction fragments to high specific activity. Analytical Biochemistry 132, 6-13.

Granados, R. R. and Williams, K.K. (1986). In vivo infection and replication of baculoviruses. pp. 89-108. In: Granados, R.R. and Federichi, B.A. eds. The biology of baculoviruses Volume I biological properties and molecular biology. CRC Press, Inc., Boca Raton, Florida USA.

Hager, D.A and Burgess, R.R. (1980). Elution of proteins from sodium dodecyl sulfate-polyacrylamide gels, removal of sodium dodecyl sulfate, and renaturation of enzymatic activity: results with sigma subunit of *Escherichia coli* RNA polymerase, wheat germ DNA topoisomerase, and other enzymes. Analytical Biochemistry 109, 76-86.

Henikoff, S. (1984). Unidirectional digestion with exonuclease III creates targeted breakpoints for DNA sequencing. Gene 28, 351-359.

Kleid, D.G., Yanasura, D., Small, B., Dowbenko, D., Moore, D.M., Grubman, M.J., McKercher, P.D., Morgan, D.O., Robertson, B.H., and Bachrach, H.L. (1981). Cloned viral protein for foot-and-mouth disease: responses in cattle and swine. Science 241, 1125-1129.

Kozak, M. (1986). Point mutations define a sequence flanking the AUG initator codon that modulates translation by eukaryotic ribosomes. Cell 44, 283-292.

Kuzio, J., Rohel, D.Z., Curry, C.J., Krebs, A., Carstens, E.B. and Faulkner, P. (1984). Nucleotide sequence of the p10 polypeptide gene of *Autographa californica* nuclear polyhedrosis virus. Virology 139, 414-418.

Kyte, J. and Doolittle, R.F. (1982). A simple method for displaying the hydropathic character of a protein. Journal of Molecular Biology 157, 105-132.

Laemmli, U.K. (1970). Cleavage of structural proteins during the assembly of the head of bacteriophage T4. Nature (London) 227,

680-685.

Leisy, D.J., Rohrmann, G.F., Beaudreau, G.S. (1984). Conservation of genome organization in two multicapsid nuclear polyhedrosis viruses. Journal of Virology 52, 699-702.

Leisy, D.J., Rohrmann, G.F., Nesson, M., and Beaudreau, G.S. (1986). Nucleotide sequence and transcriptional mapping of the p10 gene region of the *Orgyia pseudotsugata* multicapsid nuclear polyhedrosis virus. Virology 153, 157-167.

Lote, C.J. and Weiss, J.B. (1971). Identification of digalactosylcysteine in a glycopeptide isolated from urine by a new preparative technique. FEBS Letters 16, 81-85.

Maniatis, T., Fritsch, E.F., and Sambrook, J. (1982). Molecular cloning: a laboratory manual. Cold Spring Harbor Laboratory, Cold Spring Harbor, N.Y.

McClintock, J.T., Dougherty, E.M., and Weiner, R.M. (1986). Protein synthesis in gypsy moth cells infected with a nuclear polyhedrosis virus of *Lymantria dispar*. Virus Research 5, 307-322.

Minion, F.C., Coons, L.B., and Broome, J.R. (1979). Characterization of the polyhedral envelope of the nuclear polyhedrosis virus of *Heliothis virescens*. Journal Invertebrate Pathology 34, 303-307.

Oellig, C., Happ, B., Muller, T., & Doerfler, W. (1987). Overlapping sets of viral RNAs reflect the array of polypeptides in the EcoR1 J and N Fragments (map positions 81.2 to 85.0) of the *Autographa californica* nuclear polyhedrosis virus. Journal of Virology 61, 3048-3057.

Pearson, M.N., Quant-Russell, R.L., Rohrmann, G.F., and Beaudreau, G.S. P39, a major baculovirus structural protein: Immunocytochemical characterization and genetic location. Virology 167, 407-413.

Quant, R.L., Pearson, M.N., Rohrmann, G.F., and Beaudreau, G.S. (1984). Production of polyhedrin monoclonal antibodies for distinguishing two *Orgyia pseudotsugata* baculoviruses. Applied Environmental Microbiology 48, 732-736.

Quant-Russell, R.L., Pearson, M.N., Rohrmann, G.F., and Beaudreau, G.S. (1987). Characterization of baculovirus p10 synthesis using monoclonal antibodies. Virology 160, 9-19.

Rohrmann, G.F., (1986). Polyhedrin Structure. Journal of General Virology 67, 1499-1513.

Sanger, F., Coulson, A.R., Barrell, B.G., Smith, A.J.H. and Roe,

B.A. (1980). Cloning in single stranded bacteriophage as an aid to rapid DNA sequencing. Journal of Molecular Biology 143, 161-178.

Spindler, K.R., Rosser, D.S.E. and A.J.Berk. (1984). Analysis of adenovirus transforming proteins from early regions 1A and 1B with antisera to inducible fusion antigens produced in *Escherichia coli*. Journal of Virology 49, 132-141.

Tollefson, A.E. and Wold, W.S.M. (1988). Identification and gene mapping of a 14,700-molecular-weight protein encoded by region E3 of group C adenoviruses. Journal of Virology 62, 33-39.

Vlak, J.M., & Rohrmann, G.F. 1985. The Nature of Polyhedrin. Pp. 489-544. In: Maramorosch, K. and Sherman, K.E. eds. Viral Insecticides for Biological Control. Academic Press, Orlando, FL USA.

Volkman, L.E. (1986). The 64K envelope protein of budded *Autographa californica* nuclear polyhedrosis virus. Current Topics in Microbiology and Immunology 131, 103-117.

Weiss, J.B., Lote, C.J., and Bobinski, H. (1971). New low molecular weight glycopeptide containing triglucosylcysteine in human erythrocyte membrane. Nature New Biology 234, 25-26.

Whitt, M.A. and Manning, J.S. (1988). A phosphorylated 34-kDa protein and a subpopulation of polyhedrin are thiol linked to the carbohydrate layer surrounding a baculovirus occlusion body. Virology 163, 33-42.

Wilson, M.E., Mainprize, T.H., Friesen, P.D., and Miller, L.K. (1987). Location, transcription, and sequence of a baculovirus gene encoding a small arginine-rich polypeptide. Journal of Virology 61, 661-666.

Chapter III

Characterization of the Genetic Organization of the HindIII-M Region of the Multicapsid Nuclear Polyhedrosis Virus of Orgyia pseudotsugata Reveals Major Differences Among Baculoviruses

by

Adrian F. Gombart, George F. Rohrmann, Gary W. Blissard, and George S. Beaudreau

Oregon State University

Department of Agricultural Chemistry

May 8, 1989

In Press: Journal of General Virology

Characterization of the Genetic Organization of the HindIII-M Region of the MNPV of Orgyia pseudotsugata Reveals Major Differences Among Baculoviruses

ABSTRACT

A region including the 4 kb HindIII-M fragment of the multicapsid nuclear polyhedrosis virus of Orgyia pseudotsugata (OpMNPV) genome was sequenced, transcriptionally mapped, and compared to the homologous region in the MNPV of Autographa californica (AcMNPV). Five open reading frames (ORFs) oriented in the same direction were identified and were found to be expressed at late times post infection. The mRNAs from the five ORFs were found to coterminate at a single site downsteam of ORF 5. The conserved late gene promoter/mRNA start site sequence (A/GTAAG) was present upstream of all the ORFs, but did not appear to be the major site of mRNA initiation for two of the ORFs as determined by primer extension analysis. These data indicated that use of this signal for transciptional initiation may vary between different ORFs. The predicted amino acid sequences between AcMNPV and OpMNPV were compared and amino acid homologies of 26-72% for the five ORFs were observed. The comparison revealed a number of major differences in the genomes of the two viruses. A putative transposable element of 634 nucleotides was found to be inserted into the AcMNPV ORF 1 sequence reported by Oellig et al (1987). In addition, it was found that a region corresponding to the 4 kb HindIII-K/EcoRl-S/hr5 region of AcMNPV was not present in the OpMNPV genome.

INTRODUCTION

Baculoviruses comprise a diverse group of pathogens infectious for arthropods, particularly lepidopteran insects. Over 500 species of insects have been reported to be infected with baculoviruses, which include members of the occluded subgroups A (nuclear polyhedrosis viruses, NPVs); B (granulosis viruses, GVs) and the non occluded subgroup C (Martignoni and Iwai, 1986). Although all baculoviruses have a double stranded, supercoiled DNA genome packaged in a rod-shaped enveloped nucleocapsid, the size of the genomes varies considerably (88-153 kb) (Burgess, 1977; Schafer et al, 1979), and very limited DNA sequence homology is evident between many baculovirus isolates (Smith and Summers, 1982; Rohrmann et al, 1982). In addition, there is considerable diversity in the viral infectivity spectrum for host insects with many demonstrating a very narrow host range (e.g. see Crook, 1981). Despite the evident diversity of baculoviruses, little is known about the genetic relationships existing between different members. A series of investigations have compared the relatedness of the genomes of the multicapsid NPV of Orgyia pseudotsugata (OpMNPV) and the MNPV of Autographa californica (AcMNPV). It was initially observed that the two viruses possess over 24% DNA sequence homology when DNA-DNA hybridization was done under non-stringent conditions (Rohrmann et al, 1982). Subsequent hybridization of cosmid clones representing different regions of the OpMNPV genome to blots of AcMNPV DNA demonstrated that the genomes of the two viruses are organized in a colinear manner (Leisy et al, 1984). Recently, Bicknell et al (1987) reported that the OpMNPV genome lacked the homologous repeat sequences (hrs) which have been implicated as enhancers of delayed early genes in AcMNPV (Guarino and Summers, 1986).

In this report, we focus on the HindIII-M region of the OpMNPV genome which comprises 4 kb of DNA located upstream of the p26-p10-p74 gene complex. We recently demonstrated that an ORF in the OpMNPV HindIII-M region encodes a polyhedral envelope (PE) protein (Gombart et al, 1989). This protein is homologous to the AcMNPV polyhedral envelope protein recently described by Whitt and

Manning (1988) and may be bound by thiol linkages to the polyhedral envelope. The gene encoding the OpMNPV polyhedral envelope protein demonstrated 58% amino acid identity to the AcMNPV ORF 3 gene reported at 83 map units by Oellig et al (1987). The area surrounding the AcMNPV ORF 3 is well-characterized and contains a series of five ORFs in the same orientation which appear to be transcribed in an overlapping set of mRNAs which coterminate near the end of the fifth ORF. In the investigations outlined in this report, we describe the sequence and transcriptional organization of the HindIII-M region of OpMNPV.

MATERIALS AND METHODS

Insect cell lines and virus

The Lymantria dispar cell line and the production of OpMNPV have been described previously (Quant-Russell et al., 1987). For the work described in this paper, cell monolayers were infected with second passage OpMNPV at a moi of ≥ 5.

Cloning and DNA sequencing

The HindIII-M region was sequenced using appropriate restriction enzyme fragments and exonuclease III deletion mutants produced using the method of Henikoff (1984). Both M13 and plasmid sequencing were performed by the chain termination method of Sanger et al. (1980) using [α-^{35}S]dATP (New England Nuclear) and Sequenase (United States Biochemical). The plasmids pUC-18, pUC-19 and the M13 strains mp18 and mp19 were used for cloning and sequencing. A vector pBS(-) (Stratagene Cloning Systems), modified to contain a BglII site in the polylinker, was also used. This modified vector is 3216 nt in length.

RNA isolation

Isolation of total and poly (A+) RNA from OpMNPV-infected *L. dispar* cells for Northern hybridization, primer extension and S1 nuclease analysis was described previously (Blissard et al., 1989).

Northern hybridization analysis

Northern blotting of viral mRNAs, production of cRNA transcripts, prehybridization, and hybridization of the blots was carried out as described by Blissard et al. (1989). Briefly, oligo dT-selected poly(A^+) RNA isolated from OpMNPV-infected *Lymantria dispar* cells at 24 hours post infection (hpi) was electrophoresed on

1.25% agarose, 6% formaldehyde gels. The Northern hybridization probe was produced by cloning a HincII restriction fragment from within ORF 5 into the transcription vector pBS (-). cRNA transcripts were labeled with ^{32}P-UTP using T3 RNA polymerase according to the vector manufacturer's instructions. Approximately 1.0 x 10^6 cpm/ml of labeled cRNAs were used for Northern hybridization.

Primer extension and S1 nuclease analysis

In order to identify transcription start sites for ORFs 2-5, 17-mer oligonucleotides complementary to the mRNA for each ORF were synthesized and used in primer extension analysis. The location and sequence of each primer is shown in Fig. 2. Primer extension analyses were performed essentially as described by Blissard et al. (1989), except total RNA was used. Briefly, each oligonucleotide was 5' end-labeled with [gamma-^{32}P]dATP (5000 Ci/mmol) and 15 units of T4 polynucleotide kinase at 37°C for 30 min. Each labeled oligonucleotide (1 ng) was mixed with 20 μg of total RNA from uninfected or infected cells in a 10 μl annealing reaction (250 mM KCl, 10 mM Tris, pH 8.3). The mixture was heated at 80°C for 3 min and then allowed to anneal at 45°C (55°C for the ORF 5 reaction) for 45 min. For primer extension, the entire annealing reaction was used in a 30 μl primer extension reaction consisting of 12 mM Tris (pH 8.3), 8 mM $MgCl_2$, 4 mM DTT, 0.2 mM dATP, 0.2 mM dCTP, 0.2 mM dTTP, 0.4 mM dGTP, 200 units of MMLV reverse transcriptase (BRL, Inc.) and 100 μg/ml actinomycin-D. The reaction was incubated at 45°C for 45 min and terminated by adding 3 μl 3 M NaOAc and 300 μl absolute EtOH. After precipitating at -20°C overnight, the reaction mix was pelleted, resuspended in 6 μl of 0.1 M NaOH and 1 mM EDTA and incubated for 25 min at room temperature (RT). To each 6 ul sample, 4 ul of stop buffer (95% formamide, 20 mM EDTA, 0.05% bromophenol blue and 0.05% xylene cyanol FF) was added. Primer extension products were analyzed on 8% polyacrylamide, 7 M urea gels.

In order to identify the 3′ termini of the HindIII-M transcripts, S1 nuclease protection experiments were performed using probes specific for transcripts running through ORFs 2,3, and 5 (Fig. 4d) using methods described by Flavoro et al., (1980). All probes used for S1 nuclease protection analysis were 3′ end-labeled with [α-^{32}P]dATP or dCTP by using the Klenow fragment of *E. coli* DNA polymerase (Maniatis et al, 1982). For the ORF 2 probe, a pUC 19 recombinant containing the entire HindIII-M fragment was cleaved at the Asp718 site located 269 nt upstream of the ORF 2 termination codon at nt 950 (Fig. 2, Fig. 4d) and at a downstream Asp718 site located in the pUC 19 polylinker. The 3560 nt (3522 nt insert, 38 nt vector) Asp718 fragment was gel-purified and 3′ end-labeled. For the ORF3 probe, a 2682 nt BglII-HindIII fragment (nt 1518-4200, Fig. 2; Fig.4d) was subcloned into the BglII/HindIII sites of a pBS (-) vector modified to contain a BglII site in its polylinker. The recombinant was digested with BglII, 3′ end-labeled, and gel-purified. This resulted in a 5857 nt fragment (3175 nt vector plus 2682 insert) labeled at the BglII site which is located 369 nt upstream from the termination codon of ORF 3 (Fig. 2, 4d). For the ORF 5 probe, a 477 nt SalI-HindIII fragment containing 143 nt of the 3′ region of ORF 5 (Fig. 2, Fig. 4d) was subcloned into pBS (-) cut with SalI and HindIII. The subclone was digested with SalI and 3′ end-labeled resulting in a 3670 nt fragment (3193 nt vector plus 477 nt insert) (Fig. 4d). For each S1 nuclease protection experiment, 10 μg total RNA from each time point post infection (pi) of L.dispar cells and approximately 5,000 cpm probe DNA were suspended in 20 μl S1 hybridization buffer [80% formamide, 40 mM piperazine-N,N′-bis(2-ethanesulfonic acid) (pH6.4), 1 mM EDTA, 0.4 M NaCl]. The DNA-RNA mixture was then heated for 15 min at 85°C and hybridized for 3 or more hours at 60°C for the Asp718-3.6 kb and HindIII/BglII-2.68 kb probes or 7 hours at 49 C for the HindIII/SalI 477 bp probe (annealing temperatures were determined as described by Sharp et al, 1980). After hybridization, 300 μl of S1 nuclease digestion buffer (0.28 M NaCl, 50 mM sodium acetate (pH4.4), 4.5 mM $ZnCl_2$, 20 μg/ml denatured salmon testes DNA, 0.6 U/μl S1 nuclease) was added and the

resulting solution was incubated at 37°C for 30 min. 75 μl S1 termination buffer (2.5 M ammonium acetate, 50 mM EDTA) was then added and nucleic acids were precipitated by the addition of 2 volumes of ethanol. The S1 protected fragments were electrophoresed on 8% polyacrylamide-urea gels or 1% agarose gels. Agarose gels were transferred to GeneScreen Plus by capillary blot and visualized by autoradiography.

RESULTS and DISCUSSION

Nucleotide Sequence of the HindIII-M Region

Restriction fragments and exonuclease III deletion mutants from the HindIII-M region (Fig. 1) were cloned into M13 and pBS (-) and sequenced (Fig. 2). From the sequence analysis, we identified five ORFs (ORFs 1-5) (Fig. 1, 2) in the same orientation and with limited intergenic regions ranging from 4 to 43 nucleotides (nt). The ORFs varied in size from 309 to 1272 nt encoding proteins of 11.5 to 47.3 kda (see Table 1). The ORF 1 coding region begins in the HindIII-E region and terminates in the HindIII-M region at nt 626 (Fig. 1, 2). ORF 3 encodes a polyhedral envelope (PE) protein and is described in detail elsewhere (Gombart et al, 1989). The 5′ flanking region of each complete open reading frame contains the A/GTAAG consensus sequence at various distances from the translation start (ATG) (Fig. 2, 3). This sequence has been implicated in specifying the initiation and/or affecting the levels of transcription of baculovirus late genes (Rohrmann, 1986; Possee and Howard, 1987). The nucleotides at positions -3 and +4 surrounding the translation start codon of ORFs 1-3 contain a purine base (Fig. 3) indicating they conform to Kozak's rules (PuNNATGPu) for efficient eukaryotic translation initiation (Kozak, 1986). ORFs 4 and 5 have a purine at the -3 position and a pyrimidine at the +4 position. A single 3′ processing/polyadenylation signal (AATAAA) was found in the HindIII-M region at nt 3842, approximately 20 nt upstream of the termination codon of ORF 5 (Fig.2).

Mapping of the 3′ termini of the HindIII-M transcripts

To determine the site of termination of mRNAs from the HindIII-M region, three different restriction fragments were used for mapping the mRNA terminii of transcripts running through ORFs 2,3, and 5 (Fig. 4d). For ORF 2, the 3′ end-labelled 3560 nt Asp718 probe yielded an S1 nuclease-protected fragment of approximately 3200 nt (Fig.4a). For ORF 3, the 3′ end-labelled 5857 nt BglII fragment (vector plus insert) yielded an S1 nuclease-protected

fragment of approximately 2360 nt (Fig 4b). These results suggested that the mRNAs from ORFs 2 and 3 were co-terminating downstream of ORF 5 (Fig. 4d). Therefore, it appeared that OpMNPV produced a series of overlapping, coterminating mRNAs similar to those observed by Oellig et al (1987) in AcMNPV. To precisely determine the 3' termination site for the overlapping mRNAs from the region, a clone containing the 477 nt SalI-HindIII fragment which included 143 nt of the 3' region of ORF 5 (Fig. 2) was 3' end-labelled, and the resulting 3670 nt fragment (vector plus insert) (Fig. 4d). was used in S1 protection experiments. Four S1 nuclease-protected fragments of 178-181 nt were detected at 24-48 hpi (Fig.4c). From these three sets of S1 nuclease protection experiments, the 3' termini for the HindIII-M ORF 1-5 transcripts were mapped to four nt at 3900-3903 (Fig. 2). The only 3'processing/polyadenylation consensus sequence (AATAAA) in the HdIII-M region is located within ORF 5 about 50 nt upstream of the 3' mRNA termination site. A related sequence (AATAAT) is located 16 nt upstream of the termination site.

Primer extension analysis to locate transcription initiation sites

To locate the transcriptional start sites of the mRNAs, 17-mer DNA oligonucleotides complementary to sequences near the 5' ends of ORFs 2-5 were synthesized (for location and sequence of the oligomers, see Fig. 2) and were used for primer extension analysis of total RNA from infected and uninfected *L. dispar* cells. The exact location of each transcriptional start site was established by comparing the size of the primer extension products with M13mp18 sequencing ladders. The results of the primer extension analyses are shown in Fig.5a-c and summarized in Table 2. For accurate sizing of larger primer extension products, gels were run for longer periods of time (data not shown). Using an oligonucleotide complementary to the 5' region of ORF 2 for primer extension, we identified the transcription start site for both ORF 2 and ORF 1. The primer extension product for ORF1 was not precisely measured but estimated to be about 675 nt (Fig. 5a) which corresponds to an mRNA start site at approximately nt 10 (Fig. 2) and places it near the

GTAAG sequence. This indicates that at least a portion of the message for ORF 1 is transcribed through ORF 2. In addition, a major set of primer extension products of 60-61 nt (Fig. 5a) corresponding to mRNA start sites at nt 624-625 are found within the ATAAG located immediately upstream ORF 2 (Table 2, Fig. 2, 3). Primer extension from within ORF 3 resulted in products corresponding to the major ORF 2 and ORF 3 start sites indicating that at least a portion of the ORF 2 mRNA is transcribed through ORF 3. One of the ORF 3 mRNA start sites corresponds to a set of five primer extension products (71-81 nt) initiating at nt 948-958 (Fig. 2, Table 2) located near the ORF 3 ATAAG (Fig. 3). Major primer extension products of ORF 4 were localized to four regions on the sequence and the primer extension products of 60-61 nt correspond to mRNA starts sites at nt 1854-1855 (Fig. 2) on the HindIII-M sequence and are located at the T and A within the ORF 4 ATAAG (Fig. 3). ORF5 had major primer extension products of 35-36 nt corresponding to initiation at nt 2583-2584 (Fig. 2). Only a very weak start site at the G in the ATAAG for ORF 5 was observed. No primer extension products were detected for any of the primers when annealed to mRNA from uninfected cells.

Although the mRNAs from the five ORFs in the HindIII-M region coterminate downstream of ORF5, the regulation of the initiation of transcription appears to be complex. The sequence A/GTAAG is located upstream of each of the five ORFs in the HindIII M region. In two of the genes (ORFs 3 and 5), however, the major mRNAs do not appear to initate within this sequence (Fig. 2, 5). Initiation of mRNA transcription of ORF 3 occurs at a number of positions near its ATAAG, which is in contrast to initiation at one or two contiguous nt within the ATAAG motif as is often observed (e.g. ORFs 2 and 4, Fig. 3). This suggests that there may be functional constraints preventing high levels of transcription initiation from the ORF 3 ATAAG. Similarly the ATAAG upstream of ORF 5 appears to be only a minor initiation site (Fig. 5). The highest relative concentration of primer extension products of ORFs 3, 4 and 5 was in higher molecular weight products. This was especially evident in ORF 3,

where only a small fraction of the products initiated near ORF 3, and in ORF 5, which also showed a high concentration of higher molecular weight products ranging in size from 386 to over 550 nt (Fig. 5).

Northern blot analysis of HindIII-M transcription

To further investigate the transcriptional expression of the HindIII-M region, a HincII fragment from within ORF 5 was subcloned into plasmid pBS (-) (see Fig. 5c). A labelled cRNA transcript (complementary to the mRNA encoding ORF 5) was synthesized and hybridized to Northern blots of poly (A+) RNA isolated from OpMNPV-infected cells at 24 hpi (Fig. 5b). The Northern blot was exposed for varying times to allow identification of bands of differing intensity. The following summarizes the size in nucleotides of the transcripts identified by the ORF 5 cRNA probe and the likely corresponding ORF immediately downstream of the 5′ end of the transcript as predicted from the 5′ and 3′ mapping data (Table 2, Figs. 4,5): 3900 (ORF 1), 3200 (ORF 2), 2900 (ORF 3), 2400 and 2000 (ORF 4) and 1300-1600 (ORF 5). The transcripts in the 1500-1600 range are likely representative of the broad range of higher molecular weight ORF 5 primer extension products (Fig. 5b, Table 2). The data from these experiments confirmed the presence of transcripts of similar size to those determined from 5′ and 3′ mapping (Fig. 5, Table 2).

Time course of mRNA expression

Primer extension analysis was done on ORF 3 (the polyhedral envelope protein, Gombart et al, 1989) with total RNA isolated from 0-72 hpi (Fig. 5a). Specific mRNA was initally observed at 24 hpi and was present in high concentrations through 48 hpi but was at low levels at 60 and 72 hpi. This corresponds to the appearance of the polyhedral envelope (ORF 3) protein as observed by immunoblot and immunofluorescence studies of infected cells (Gombart et al, 1989). The other ORFs appeared to be expressed in a similar manner with no primer extension products observed at 12 hpi and strong expression

observed at 24 hpi.

Comparison of OpMNPV HindIII-M region with the homologous region in AcMNPV

In a previous study (Gombart et al, 1989), we demonstrated that the OpMNPV 32 kDa polyhedral envelope-associated protein and the AcMNPV ORF 3 (Oellig et al., 1987) shared 58% amino acid identity. It was also observed that the AcMNPV polyhedral envelope protein has a series of 16 ARG-SER repeats, not present in the OpMNPV ORF, making the AcMNPV protein significantly larger. Comparison of the OpMNPV and AcMNPV predicted amino acid sequences from ORFs 1, 2, 4, and 5 demonstrated sequence similarities varying from 26-72% (Fig. 6 and Table 1). Other related proteins derived from OpMNPV and AcMNPV sequence data are also included in Table 1. They indicate that ORF 4 at 26% similarity is the least conserved, whereas polyhedrin at 90% similarity is the most highly conserved.

In addition to the ARG-SER repeats in ORF 3 of AcMNPV described above, a number of other major differences between the two viruses were observed (Fig. 7). Amino acid sequence comparison between the two ORF 1 sequences revealed the existence of a 634 nt insert one nt after the codon for amino acid residue 101 (Fig. 6) in AcMNPV. Analysis of this insert revealed 4 base pair (bp) direct repeats (TTAA) flanking 14 bp inverted repeats on either end of the inserted DNA. This motif of inverted repeats flanked by direct repeats is characteristic of transposable elements found in both eucaryotic and procaryotic systems (Lewin, 1985). The direct repeat sequence is commonly a duplication of viral/host sequence upon insertion of foreign DNA. This particular sequence (TTAA) has been found duplicated at a number of sites where insect DNA has been inserted into a baculovirus genome (Fraser et al, 1985; Carstens, 1987; Beames and Summers, 1988). This putative transposable element located in ORF 1 contains the EcoR1 site (Fig. 7) which causes the restriction map alterations characteristic of this strain of AcMNPV (Oellig et al, 1987). A search for open reading frames within the nucleotide sequence of the putative transposable element indicated

that none existed although a small or spliced gene cannot be ruled out.

Such transposable elements appear to be derived from repeated DNA in the host insect cell (Beames and Summers, 1988). Although they appear to lack open reading frames, it is evident they could have important influences on viral evolution. In the AcMNPV strain used by Oellig et al (1987), the transposon contains the sequence ATAAG which has been implicated as a regulatory element of baculovirus late genes (Rohrmann, 1986; Possee and Howard, 1987). Oellig et al report a transcript originating near this sequence within the transposon. The first ATG contained within such an mRNA could result in the translation of the 3' half of the ORF 1 polypeptide. In addition, the solo LTR remaining after the excision of a retrotransposon in AcMNPV, contained two bidirectionally oriented ATAAG sequences which appear to cause the initation of late transcripts (Friesen et al, 1986). Therefore, in addition to disrupting viral genes, the insertion of transposable elements could also cause them to be expressed in an aberrant manner. In order to align the region upstream of the transposon insertion in the AcMNPV ORF 1 with OpMNPV, three changes had to be made in the sequence of Oellig et al (1987) (these changes are described in the legend to Figure 6) indicating that the upstream region of ORF 1 of this AcMNPV strain has evolved into a pseudogene, whereas in the OpMNPV genome and another AcMNPV strain (see legend Fig. 6), the upstream region of ORF 1 appears to be functional and conserved. Most transposable elements reported in the AcMNPV genome have been detected because they produce a 'few polyhedra' (FP) phenotype which is detectable by examination of plaques and are often associated with alterations in the HindIII-I fragment of the AcMNPV (Beames and Summers, 1988). The detection of such an element in ORF 1 suggests that the incorporation of transposable elements in baculovirus genomes may occur over a greater region of the genome than the FP detection system indicates. Such mutants would not normally be evident because of the lack of a suitable detection system.

When the OpMNPV HindIII-M and the contiguous p26-p10-p74 region

was aligned with sequence data for the similar region of AcMNPV, it was observed that the OpMNPV genome lacks approximately 4 kb of DNA corresponding to the AcMNPV HindIII-K/EcoRI-S/hr5 region (Fig. 7). This region is located between ORF 5 and the p26 gene in AcMNPV. In OpMNPV, the p26 gene and ORF 5 are separated by an intergenic region of 224 bp (Fig. 2). In order to determine whether a region homologous to the AcMNPV HindIII-K/EcoRI-S region exists elsewhere in the OpMNPV genome, two hybridization experiments were performed using labelled AcMNPV HindIII-K and EcoRI-S fragments. The two AcMNPV fragments were labelled to high specific activity (Feinberg and Vogelstein, 1984) and were hybridized under non-stringent conditions (30% formamide) (Maniatis et al, 1982) to blots of digested OpMNPV cosmid DNA and total viral genomic DNA. No hybridization was detected for either probe (data not shown). This suggests that regions homologous to the AcMNPV HindIII-K and EcoRI-S fragments do not exist in the OpMNPV genome.

In AcMNPV, the HindIII-K/EcoRl-S/hr5 region contains, in addition to hr5, two ORFs encoding predicted proteins of 35 and 94 kd (Friesen and Miller, 1987). These ORFs appear to be expressed as delayed-early genes and lack the baculovirus ATAAG putative late gene regulatory sequence. Their mRNA is initiated downstream of a TATA-like consensus sequence. Baculoviruses likely have a number of groups of genes whose functions are essential for their replication and survival in the environment (genes involved in DNA replication, viral structure, assembly, and etc.) as well as genes which are not absolutely essential but confer a selective advantage. The bacteriophage T4, which has a genome size similar to baculoviruses (160 kb), codes for over 140 proteins. Of these, nearly half have been found to be non-essential for phage production (Lewin, 1985). Many of the non-essential genes encode proteins involved in metabolism of DNA precursors and in the regulation of translation. The two ORFs in the AcMNPV HindIII-K/EcoRl-S region may represent such non-essential genes; these may confer a selective advantage to the virus, but without which other baculoviruses such as OpMNPV can survive. Therefore, the large difference in genome sizes of

occluded baculoviruses (88-153 kb) (Burgess, 1977; Schafer et al, 1979) may reflect the incorporation of genes from insects or other viruses and may give the virus a selective advantage but are not essential for its replication.

Table I: Comparison of Baculovirus Proteins[a]

ORF		# of a.a.	MW (kDa)	% Identity DNA	% Identity Amino Acid
ORF 1[b]	Op	193	21.2	ND[c]	64
	Ac	199	22.1		
ORF 2	Op	103	11.5	69	72
	Ac	106	12.1		
ORF 3	Op	297	32.4	62	58
	Ac	322	36.5		
ORF 4	Op	228	25.9	27[d]	26
	Ac	219	25.1		
ORF 5	Op	424	47.3	58	53
	Ac	419	48.3		
p10	Op	92	10	54	41
	Ac	94	10.1		
p26	Op	229	26	55	47
	Ac	240	26		
p74[e]	Op	158	-	71	70
	Ac	158	-		
PH	Op	245	28.9	80	90
	Ac	245	28.7		

[a] For references see legend Fig. 7.

[b] The sources for the complete ORF 1 sequence are described in the legend Fig. 6.

[c] This comparison was not done because an uninterrupted ORF 1 DNA sequence from a single strain of AcMNPV is unavailable.

[d] Not significant homology.

[e] The nucleotide sequences for the p74 ORF are not completed at present and the partial predicted amino acid sequence are compared.

TABLE 2

TRANSCRIPT SIZE DETERMINED BY 5' AND 3' MAPPING

LOCATION OF PRIMER	SIZE (NT) PRIMER EXTENSION PRODUCT	LOCATION PRIMER EXTENSION PRODUCT ON SEQUENCE (FIG.2)	DOWNSTREAM[a] ORF	PREDICTED TRANSCRIPT SIZE[b]
ORF 2	~675[c]	~9	ORF 1	3900
	60-61	623-624	ORF 2	3280
ORF 3	405-406, 276, 257	623-624, 753, 772	ORF 2	3280, 3140, 3120
	154-155, 71-81	874-875, 948-958	ORF 3	3030, 2950
ORF 4	322, 301, 122-123,	1593, 1614, 1792-1793	ORF 4	2400, 2300, 2110
	60-61	1854-1855		2050
ORF 5[d]	~386-550	~2066-2233	ORF 5	~1530-1670
	35-36	2583-2584	ORF 5	1320

[a]Because of the overlapping nature of the HindIII-M transcripts, some primer extension products which were primed within ORF 2 and 3 extended through the preceding ORF and therefore mapped to the 5' flanking sequence of the upstream ORF.

[b]Because of the heterogeneity at the 5' and 3' ends of the mRNAs the sizes are rounded off to the nearest 10 nt.

[c]These Sizes and locations are estimated from long gel runs and are not determined to the nucleotide.

[d]The higher molecular weight ORF 5 transcripts are derived from estimates of longer electrophoresis runs of the primer extension samples from Fig. 5a.

Fig. III. 1. Location of the OpMNPV HindIII-M region. a) HindIII restriction enzyme map of the OpMNPV genome indicating the location of polyhedrin (PH) and p39 genes. b) Restriction map of the HindIII M and Q region indicating the location of ORFs 1-5 and the genes for p26, p10 and p74. Abbreviations: A, Asp718; Bg, BglII; C, ClaI; H, HindIII; K, KpnI; P, PstI; S, SalI; Ss, SstI; X, XhoI.

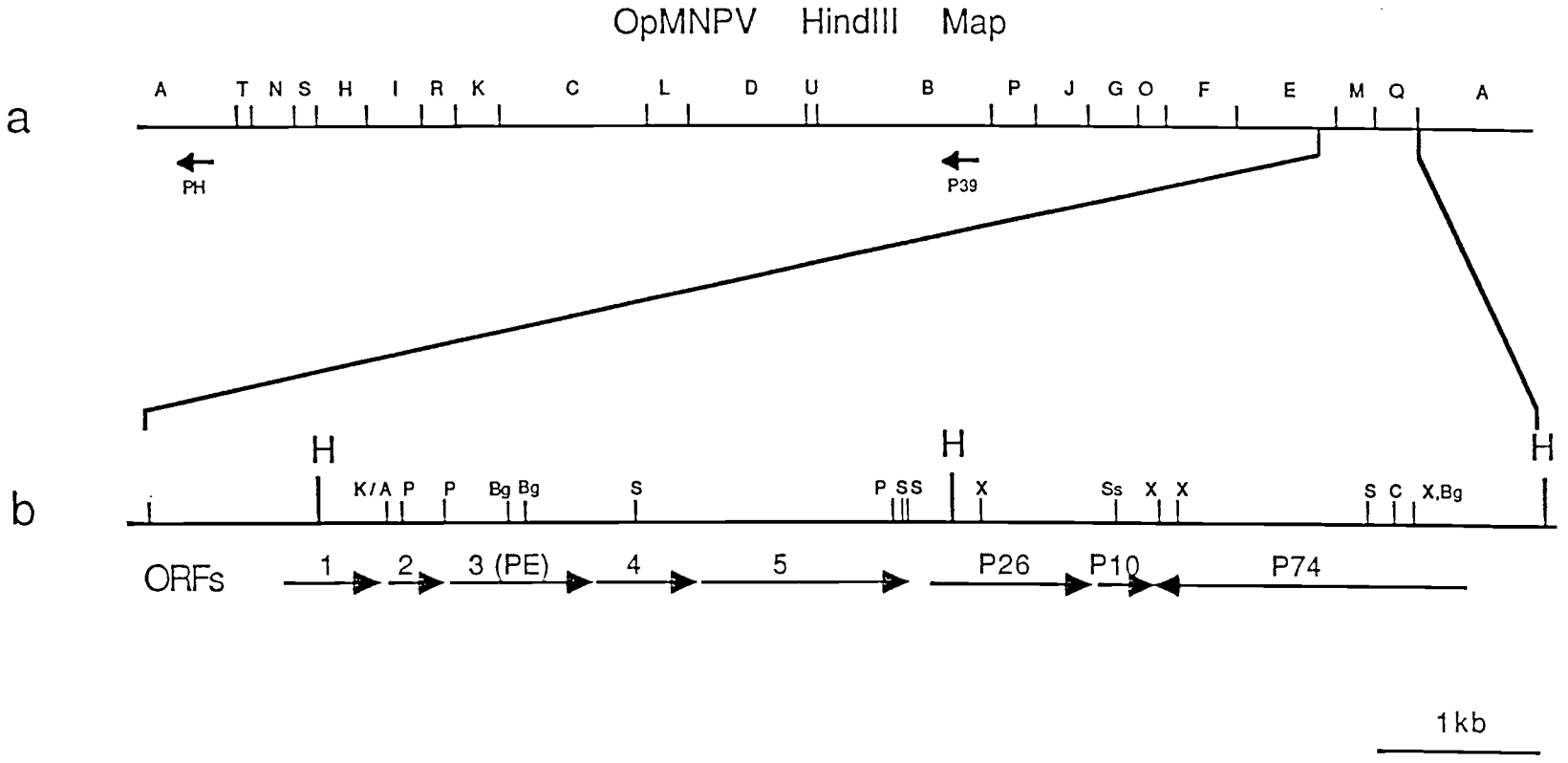
OpMNPV HindIII Map
a
A T N S H I R K C L D U B P J G O F E M Q A
PH
P39
b
H H H
K/A P P Bg Bg S P S S X Ss X X S C X,Bg
ORFs
1 2 3 (PE) 4 5 P26 P10 P74
1kb

Figure III.1

Fig. III. 2. Nucleotide sequence of the OpMNPV HindIII-M region. The putative promoter element (A/GTAAG) upstream of ORFs 2-5, the polyadenylation signal (AATAAA) (nt 3842) and the mRNA termination site (nt 3900-3903) are underlined. The mRNA start sites are indicated with the relevant nt underlined and the translational start (ATG) sites for ORFs 2-5 and the p26 gene downstream of ORF 5 are indicated. The predicted amino acid sequence of each ORF is given below the nucleotide sequence. Major restriction enzyme sites and the location of the primers used in the primer extension analysis are underlined.

```
HincII  10          20          30          40              ORF 1
GTTAACAAAA CTTAATACTT TCTCCGCCCT AATGTAAGAC GGACATTGAC ATG GCG AAC GCC
                                                        M   A   N   A

     68          77          86          95          104         113
GAT TCG CTC GAC GCC CGC GCG TTC AGT TAC GCC CCC GAC GCC AGC TTT GAA GTG
D   S   L   D   A   R   A   F   S   Y   A   P   D   A   S   F   E   V

    122         131         140         149         158         167
ATT ATA ATC ACA AAC GCG CCC AAC GAC CAC GAC GGG TAT CTG GAG CTG AAC GCC
I   I   I   T   N   A   P   N   D   H   D   G   Y   L   E   L   N   A

    176         185         194         203         212         221
GCG GCA CGC TTG TTG GCG CCG TTT CAA AAA AAC ATA TCC GCC CTA TGG ACA AGC
A   A   R   L   L   A   P   F   Q   K   N   I   S   A   L   W   T   S

    230             HindIII 257         266         275
GCG GCG CCG TCG CAC AAG CTT GTT AGA AAC AAC AAA AAC TAT CTG CAC GTT TTT
A   A   P   S   H   K   L   V   R   N   N   K   N   Y   L   H   V   F

    284         293         302         311         320         329
GGG CTG TTT AAA TAT TTG CAA AAC TAC AAT TTC AAC GCT AAA CCG CAC CCG CCC
G   L   F   K   Y   L   Q   N   Y   N   F   N   A   K   P   H   P   P

    338         347         356         365         374         383
GAA TAC TAC ACT GTG AAA TCG GTA ATT TGC GAC CTT ATA GCG GGC GCG CAG GGC
E   Y   Y   T   V   K   S   V   I   C   D   L   I   A   G   A   Q   G

    392         401         410         419         428         437
AAA ACG TTT GAC CCG CTG TGT GAG ATC AAG ACG CAA CTG TGC GCC ATT CAA GAA
K   T   F   D   P   L   C   E   I   K   T   Q   L   C   A   I   Q   E

    446         455         464         473         482         491
AGC CTG AAC GAG GCA ATA GTG ACG TTG AAC AGC CAC GCG ACC GCC GAG CCC GCG
S   L   N   E   A   I   V   T   L   N   S   H   A   T   A   E   P   A

    500         509         518         527         536         545
CCC GGT GCG CCT TGC GAC GCG CGC GAG TTG GTC GAA ACG CTG CAT TCG GAA TAC
P   G   A   P   C   D   A   R   E   L   V   E   T   L   H   S   E   Y

    554         563         572         581         590         599
AGC CAA AAG CTG ACG TTT GCT ACC GAC ACC ATT CTG GAC AAC GTG AAA AGC ATC
S   Q   K   L   T   F   A   T   D   T   I   L   D   N   V   K   S   I

    608         617         5'                  ORF 2           655
AAG GAC CTG GTG TGC CTC AAT AAG TGAAAATTTT AGCC ATG AAT TTT TGG GCG GCT
K   D   L   V   C   L   N   K                   M   N   F   W   A   A

    664     Primer 2    KpnI/Asp718 691         700         709
TTT AGC GCG TGC TTG GTG GGG TAC CTG GTC TAC TCG GGC CGC TTG AAC GGC GAA
F   S   A   C   L   V   G   Y   L   V   Y   S   G   R   L   N   G   E

PstI            727         736         745         5'          763
CTG CAG GAG ATC AAA TCT ATT CTA ATA ATA GCG TAC GAG GCG GCG GAC AAG CGT
L   Q   E   I   K   S   I   L   I   I   A   Y   E   A   A   D   K   R
```

Figure III.2

```
      5'          781          790          799          808          817
TAC AGG GGC GTG ATC GAC GAA ATT GAG TCG CTC AAA ACG GAC ACG TTT ATG ATG
Y   R   G   V   I   D   E   I   E   S   L   K   T   D   T   F   M   M

    826          835          844          853          862          871
TTG TCG AAC TTG CAA AAC AAC ACA ATT CGC ACG TGG GAC GCC GTT GCG AAA AAC
L   S   N   L   Q   N   N   T   I   R   T   W   D   A   V   A   K   N

5'              889          898         HincII        916          925
GGC AAA AAA ATT GCC AAT TTG GAC GAG CGC GTC AAC GGG CTG CTG GCC AAG CAC
G   K   K   I   A   N   L   D   E   R   V   N   G   L   L   A   K   H

    934                  5'   5'  5'                  PstI             989
GCG GTG CCC GCG CTC GTG AGA TAAGTTATTA TCAAAACTTT GGCTGCAGCT ACAATATCAC
A   V   P   A   L   V   R

      ORF 3                          Primer 3                    1036
ACAAT ATG ACG CCC AAC AAC AAC GTA ATG TTC GAC GAC GCG TCG GTG ATG TGG
      M   T   P   N   N   N   V   M   F   D   D   A   S   V   M   W

1045        1054         1063         1072         1081         1090
ATC GAC GCC GAC TAC ATC TAC CAA AAC TCC AAA ATG CCG CTG TCC ACG TTC CAA
I   D   A   D   Y   I   Y   Q   N   S   K   M   P   L   S   T   F   Q

PvuII       1108         1117         1126         1135         1144
CAG CTG CTC TTC TCC ATT CCG TCC AAG CAT CGC AAA ATG ATC AAC GAC ATC GGC
Q   L   L   F   S   I   P   S   K   H   R   K   M   I   N   D   I   G

1153        1162         1171         1180         1189         1198
AAC CCG GCG TGC AAC CCG CCG TCG TGC TCC TTT CCG CCC AGC AAC AGC ACG GTC
N   P   A   C   N   P   P   S   C   S   F   P   P   S   N   S   T   V

1207        1216         1225         1234         1243         1252
AAG TAC ATG GTG GAC ATT TAC GGC GCG GCG GTG CTG GCG CTG CGC TGC CCG TCG
K   Y   M   V   D   I   Y   G   A   A   V   L   A   L   R   C   P   S

1261            PvuII            1288         1297         1306
CTG TTC TCC GAC CAG CTG CTA ACC ACG TTT ACT GCT AAC AAC TAC TTG AGC TAC
L   F   S   D   Q   L   L   T   T   F   T   A   N   N   Y   L   S   Y

1315        1324         1333         1342         1351         1360
TGC AAC CGC CAA CGG CCG TGC CCG CAG CCG CCG TGC CCG CAG CCG CCC TTC GAC
C   N   R   Q   R   P   C   P   Q   P   P   C   P   Q   P   P   F   D

1369        1378         1387         1396         1405         1414
TGC GCG CAA ACC CAA ATC CTG GAC GCG TTG GAA AAA CTG GCG CGC CAG AGC GAC
C   A   Q   T   Q   I   L   D   A   L   E   K   L   A   R   Q   S   D

1423        1432             BglII            1459         1468
CTG GTC GTG AAC AGC CTC AAC CAG ATC TCA CTG AAC CAA TCC AAC CAG TTT TTG
L   V   V   N   S   L   N   Q   I   S   L   N   Q   S   N   Q   F   L

1477        1486         1495         1504         1513        BglII
GAA CTG TCC AAC ACG CTG AAC ACG GTG CGC GCC CAA AAC GCG CAG ATC TTG GCG
E   L   S   N   T   L   N   T   V   R   A   Q   N   A   Q   I   L   A
```

Figure III.2
Continued

```
1531          1540          1549          1558          1567          1576
 GCG CTG GAA ACC ACC AAA GAC GCA ATC TTG ACG CGC CTC AAC GCG TTG GTG GAC
 A   L   E   T   T   K   D   A   I   L   T   R   L   N   A   L   V   D

1585          5'            1603                  5'                    1630
 GAC ATT AAA GCG GCG CTG CCC GAC CAA TCC GCC CAA CTG CAA GAA TTG GCC GAC
 D   I   K   A   A   L   P   D   Q   S   A   Q   L   Q   E   L   A   D

1639          1648          1657          1666          1675          1684
 AAG CTG CTG GAC GCA ATC AAC TCG GTC GCG CAA ACG CTT CGC GGC GAA ATG AAC
 K   L   L   D   A   I   N   S   V   A   Q   T   L   R   G   E   M   N

1693          1702          1711          1720          1729          1738
 AAC ACC AAT TCG ATT CTA ACC AAT TTG GCG TCC AGC ATC ACC AAC ATC AAC AGC
 N   T   N   S   I   L   T   N   L   A   S   S   I   T   N   I   N   S

1747          1756          1765          1774          1783              5'
 ACG TTG AAC AAC TTG CTG GCC GCC ATT GAG GGT ATA GGC GGC GAC GGC GGC GGT
 T   L   N   N   L   L   A   A   I   E   G   I   G   G   D   G   G   G

1801          1810          1819          1828          1837          1846
 CTT GGC GAC GCA GAT AGG CAA GCG CTA AAC GAG GTG CTC AGC CTG GTC ACC GAA
 L   G   D   A   D   R   Q   A   L   N   E   V   L   S   L   V   T   E

 5'                                                   ORF 4
ATA AGA AAC ATT TTG ATG GGC ACC GCT CGC AAG TAGC ATG CCC AGA GAC ACG
I   R   N   I   L   M   G   T   A   R   K       M   P   R   D   T

 Primer 4                          1928          1937          1946          1955
AAA CCG TAC AGC CGG CCG GCC AAC GCG CCG CGC CCG GGC GTT AAA ACC GAG CGC
K   P   Y   S   R   P   A   N   A   P   R   P   G   V   K   T   E   R

    1964          1973          1982          1991          2000          2009
TCA AAC CAG TTT AAA GCG GCG TCA ACC AAA TAC GGC AAA CGC GTC AAC GAC GCG
S   N   Q   F   K   A   A   S   T   K   Y   G   K   R   V   N   D   A

    2018          2027          2036          2045          2054          2063
AAC AAG GAA ACG CGC CCC GTG GCG TTC GTG GAC ATC AAG CTC AAC CAC CGC GCC
N   K   E   T   R   P   V   A   F   V   D   I   K   L   N   H   R   A

    2072          2081          2090          2099          2108          2117
ACG CCC GAA ATG GAG CAA CGG ATG CAG GCC GTG TAC GCG CGG CAA AAG CCG TCC
T   P   E   M   E   Q   R   M   Q   A   V   Y   A   R   Q   K   P   S

    2126          2135          2144          2153          2162          2171
ATA TTC AAC AAA TCC GCC GTA GCA GAG TTC ATT AAA AAT CGC ACG TTT GTG GTG
I   F   N   K   S   A   V   A   E   F   I   K   N   R   T   F   V   V

    2180          2189          2198          2207          2216          SalI
GCG TTT GCG CAC CCC ACG TAC ACG ATA CAG TTT AAC AAA ATT CCC ACC GTC GAC
A   F   A   H   P   T   Y   T   I   Q   F   N   K   I   P   T   V   D

 PvuII            2243          2252          2261          2270          2279
CAG CTG CGT GTC TAT TGT TCC AAC ATT AAC AAG GAC TTG TTG TTC AAA GAT AAA
Q   L   R   V   Y   C   S   N   I   N   K   D   L   L   F   K   D   K
```

Figure III.2
Continued

```
    2288          2297          2306          2315          2324          2333
AAC CAA CAA ATG CGA AAC GCG CTG CCC AAC GCG GCG TCA TTT CGC GTG CAA ATT
N   Q   Q   M   R   N   A   L   P   N   A   A   S   F   R   V   Q   I

    2342          2351          2360          2369          2378          2387
AAC GAC GAG CCG CTG TTT AAG GTG CAA ACC GTC GTG TAC GAC AAA GAA TCC GCC
N   D   E   P   L   F   K   V   Q   T   V   V   Y   D   K   E   S   A

            HincII                        2423          2432          2441
CAA TTG GTG TTG ACG ATA AGG TTT TTG CCC AGA CAA ACA ATG GAG CTG CTG CCG
Q   L   V   L   T   I   R   F   L   P   R   Q   T   M   E   L   L   P

    2450          2459          2468          2477          2486          2495
ATG AAA AAG TGC GTT GTA TAT CTG AAC ATA TTG TCG AAC GCG TCT GTG GAT TGG
M   K   K   C   V   V   Y   L   N   I   L   S   N   A   S   V   D   W

    2504          2513          2522          2531          2540          2549
GCA GTG CCG GCG GAT TTG CTG CGC GCG TTT GCC AAG CTG GCG CTG GCG CCG CCC
A   V   P   A   D   L   L   R   A   F   A   K   L   A   L   A   P   P

    2558                                      5'          ORF 5
ATC CCC GCG CCG CAG AAC GTT TAACGCCCCG CTTAGCC ATG CAC GCG CCG CTC ACC
I   P   A   P   Q   N   V                     M   H   A   P   L   T

 Primer 5                 2629          2638          2647          2656
GCG GAG CAG CGC GAC GTG TAC GAC AAG TAC AAG TTT GCC ACG TAC GCG CGG TCG
A   E   Q   R   D   V   Y   D   K   Y   K   F   A   T   Y   A   R   S

2665          2674          2683          2692          2701          2710
GTG GCG TTG ACG CGC GCG CAG CTC GAC CAG TGG CGC GAC AAC AAG GTT ATC GTT
V   A   L   T   R   A   Q   L   D   Q   W   R   D   N   K   V   I   V

2719          2728          2737          2746          2755          2764
CCG GAA CCC GTG TCG CGC GCA GAG ACG CTG CGC GTG GAG GCC GCC ACG CGC GGC
P   E   P   V   S   R   A   E   T   L   R   V   E   A   A   T   R   G

2773          2782          2791          2800          2809          2818
CAG AGC AAG AAC GCG CTG TGG AAC CTG CTG CGG CTG GAC CGC AGC ACC GCG TCG
Q   S   K   N   A   L   W   N   L   L   R   L   D   R   S   T   A   S

2827          2836          2845          2854          2863          2872
CGC TCG TCG GGC GGC GTC GCA CTG CGC TCG TCC GCG CTG GCG TTT GGC AAC GCG
R   S   S   G   G   V   A   L   R   S   S   A   L   A   F   G   N   A

2881          2890          2899          2908          2917          2926
CAA GAG AAC CGG CTA AAG TTG GCC AAC GGA GAG CTG TTC GAA CGG CTG GGC CGG
Q   E   N   R   L   K   L   A   N   G   E   L   F   E   R   L   G   R

2935          2944          2953          2962          2971          2980
CTG GCC GCG GAG CGC GCG GGC TGC CCC GTC GCC GAG ACG GTG CTG GAC TGC GGC
L   A   A   E   R   A   G   C   P   V   A   E   T   V   L   D   C   G

2989          2998          3007          3016          3025          3034
ATG TTT ATT AGC GCG TTT GGG CTG CAC TCG GCG TCG CCC GAC GCC TAT TTC GCT
M   F   I   S   A   F   G   L   H   S   A   S   P   D   A   Y   F   A
```

Figure III.2
Continued

```
3043          3052          3061          3070          3079          3088
 ATG GCC GAC GGC TCG TGC GTG CCC GTG GAG ATC AAG TGC CCG TTC AAC TAC CGC
 M   A   D   G   S   C   V   P   V   E   I   K   C   P   F   N   Y   R

3097          3106          3115          3124          3133          3142
 GAC ACC ACG GTG GAC CAA ATG CGC TTG GAG CTG GGT AAG GCC AAC CGC AAG TAC
 D   T   T   V   D   Q   M   R   L   E   L   G   K   A   N   R   K   Y

3151          3160          3169          3178          3187          3196
 CGC GTC AAG CAC ACG GCG CTG CTC GTC AAC AAG GCG GGC CCC GCG CAA TTT GAG
 R   V   K   H   T   A   L   L   V   N   K   A   G   P   A   Q   F   E

3205          3214          3223          3232          3241          3250
 GTG GTC AAG ACG CAC GAC CAC TAT CGG CAA ATG CAA CGG CAG ATG TAC GTG ATG
 V   V   K   T   H   D   H   Y   R   Q   M   Q   R   Q   M   Y   V   M

3259          3268          3277          3286          3295          3304
 CGC AAC GCG CCC GTG TGT TTT TAC GTG GTG CGG TTT AAA CAC AAC CTG GTG GCG
 R   N   A   P   V   C   F   Y   V   V   R   F   K   H   N   L   V   A

3313          3322          3331          3340          3349          3358
 CTG GCC GTG CCG CGC GAC GAC GAT TTT TGC CGA AAA GAA GCG GCC GCG GAG GGC
 L   A   V   P   R   D   D   D   F   C   R   K   E   A   A   A   E   G

3367          3376          3385          3394          3403          3412
 GCC GCG TTC GTG GCT TTC GCA ACG GAG AAC GCG GGG CGC GTG CAG TTT AAG CGC
 A   A   F   V   A   F   A   T   E   N   A   G   R   V   Q   F   K   R

3421          3430          3439          3448          3457          3466
 GGC GAC CGC CGC CGC GCG TCT TTT GCC CAA AAC GCC GCC GAC CAC GGA TAC AAC
 G   D   R   R   R   A   S   F   A   Q   N   A   A   D   H   G   Y   N

3475          3484          3493          3502          3511          3520
 GCC GCG CAG GTG GAC GCG CTG GTG CGC CGC GGA CTG TAT TTG TCG TAC GGG CAG
 A   A   Q   V   D   A   L   V   R   R   G   L   Y   L   S   Y   G   Q

3529          3538          3547          3556          3565          3574
 TTG CGC TGC GGG CAT TGC GAC GCG TTT GCG CTG GAC GGC CCG CGG GCG TTT GAG
 L   R   C   G   H   C   D   A   F   A   L   D   G   P   R   A   F   E

3583          3592          3601          3610          3619          PstI
 CTG GCC ATG GCG CGC CCA CAC GAA CAA TGC GAC GGG CTG GCG CTG CAG GAG CAC
 L   A   M   A   R   P   H   E   Q   C   D   G   L   A   L   Q   E   H

3637          3646          3655          3664          3673          3682      SalI
 GAG TTC GAC AAT GTT GCG TTT CTC GAT TTC ACC AAA CGC TAC ACC AGT TTG GTC
 E   F   D   N   V   A   F   L   D   F   T   K   R   Y   T   S   L   V

____          3700          3709          3718          SalI          3736
 GAC AAG CGC TGC GAC GAC GCC CGC GCA CTG CGC GTC GAC GGC TTC TAC GTG GAC
 D   K   R   C   D   D   A   R   A   L   R   V   D   G   F   Y   V   D

3745          3754          3763          3772          3781          3790
 GAC GCC GGC GCC GTG AAA ACC TTT TGT TGC GGC GTG CAC GGC AGC AAT GCG TCA
 D   A   G   A   V   K   T   F   C   C   G   V   H   G   S   N   A   S
```

Figure III.2
Continued

```
3799          3808          3817          3826          3835          Poly A signal
 CGG CGC CAC CTT CCC ACG TGT TCG TAT TAT TTA GCA ATG GGT GTA AAT AAA ATA
 R   R   H   L   P   T   C   S   Y   Y   L   A   M   G   V   N   K   I

3853          3862          3872          3882          3892          3' End mRNA
 CAA AAT AAT ATG TGATTTATTT ATTGGTAATA ATTAAAAACT GTTTGCACAA ACTTGATTTT
 Q   N   N   M

       3922          3932          3942          3952          3962          3972          3982
 TATTTCGGCA AGAACCATTC GTCCATGTAT TTGTTTGACA CGTTCGTTTT GCATTCAACC GGTTTGCACG

       3992          4002          4012          4022          4032          4042          4052
 CGTCGCTGTT TTGCGCGCAC GCAATCACAC ATATTTGTCA CATCGCTATT TAAAAGGAAA CGCGGTCGCA

      5' p26                                  p26 ORF
 AAAGCTCAAA CGTTATTTGA AACCGGCGCG CA ATG TAC ATA AAG ATG GAG GTT GAA TTT
                                     M   Y   I   K   M   E   V   E   F

4114          4123          4132          4141          4150          4159
 GAC GAA GAC ACG GGC GCC CTT CAA ATC GGC GGA CAA GAG GTG TTT GTA ATG GTG
 D   E   D   T   G   A   L   Q   I   G   G   Q   E   V   F   V   M   V

4168          4177          4186          HindIII
 TTC GAG CCC GGT CAA GAG GTT TTT GAC AAA AGC TT       4200
 F   E   P   G   Q   E   V   F   D   K   S   L
```

Figure III.2
Continued

Fig. III. 3. Nucleotide sequence of the 5′ flanking region containing the putative regulatory sequence (A/GTAAG) of each ORF. A 14-nt sequence containing the invariant A/GTAAG sequence found upstream of baculovirus late genes is set off by spaces in each sequence. The upstream location of the first nucleotide of each A/GTAAG sequence is indicated above each sequence and the mRNA start sites within this region are underlined. The ATG translational start for each ORF is underlined with the -3 and +4 nucleotide positions indicated. The consensus sequence is derived from baculovirus hyperexpressed genes (Rohrmann, 1986). The ATAAGs of ORFs 3 and 5 only weakly specified initiation as compared to other sites within the HindIII-M region.

```
                                                        -3       +4
                    -17
ORF1   CCGCCCT AATGTAAGACGGAC ATT.............. G ACATG G

                    -19
ORF2   GTGTGCC TCAATAAGTGAAAA TTT.............. G CCATG A

                    -46
ORF3   CGCTCGT GAGATAAGTTATTA TCA.............. A AAATG A

                    -37
ORF4   GGTCACC GAAATAAGAAACAT TTT..............A GCATG C

                    -184
ORF5   GGTGTTG ACGATAAGGTTTTT GCC.............. G CCATG C

Consensus      TAAATAAGTATTTT
```

Figure III.3

Fig. III. 4. Determination of the location of the 3′ ends of transcripts from ORFs 2,3 and 5 by S1 nuclease protection assays. a) S1 protection analysis of the 3′ end of mRNAs from within ORF 2. b) S1 protection analysis of the 3′ end of mRNAs from within ORF 3. c) S1 protection analysis of the 3′ end of mRNAs from within ORF 5. Numbers at top of gel indicate hpi; 'm' indicates mock infected cells; 'p' indicates untreated radioactively labelled probe. The external lanes on panels a) and b) are radioactively labelled markers. The sizes of relevant markers are indicated between panels a) and b). The numbers to the left of panel a) and to the right of panel b) indicate the size of the probe (vector plus insert) used (upper number) and the size of the protected fragment (lower number). In panel c) an M13mp18 sequencing ladder was used to determine the size of the S1 protected fragments. The numbers to the right indicate the size of the protected fragments. The autoradiogram from panels a) and b) was derived from a 1% agarose gel blotted to Gene Screen Plus. Panel c) represents an autoradiogram of an 8% polyacrylamide, 7M urea gel. d) Strategy for mapping the 3′ ends of transcipts from the HindIII-M region. Solid lines under the ORFs indicate the three probes used in the 3′ S1 analysis. The wavy line beneath each solid probe line indicates the protected fragments. The numbers at the left indicate the size of the probe (this number and the diagram indicate the viral component on the probe only) and protected fragments and asterisks indicate the position of the labelled end. Abbreviations: same as in Fig. 1 and Hp, HpaII; Pv, PvuII; Hc, HincII.

All probes used for S1 nuclease protection analysis were 3′ end-labelled with [Á-^{32}P]dATP or dCTP by using the Klenow fragment of *E. coli* DNA polymerase (Maniatis et al, 1982). For the ORF 2 probe, a pUC 19 recombinant containing the entire HindIII-M fragment was cleaved at the Asp718 site located 269 nt upstream of the ORF 2 termination codon at nt 950 (Fig. 2, Fig. 4d) and at a downstream Asp718 site located in the pUC 19 polylinker. The 3560 nt (3522 nt insert, 38 nt vector) Asp718 fragment was gel-purified and 3′ end-labelled. For the ORF3 probe, a 2682 nt BglII-HindIII fragment (nt

1518-4200, Fig. 2; Fig.4d) was subcloned into the BglII/HindIII sites of a pBS (-) vector modified to contain a BglII site in its polylinker. The recombinant was digested with BglII, 3' end-labelled, and gel-purified. This resulted in a 5857 nt fragment (3175 nt vector plus 2682 insert) labelled at the BglII site which is located 369 nt upstream from the termination codon of ORF 3 (Fig. 2, 4d). For the ORF 5 probe, a 477 nt SalI-HindIII fragment containing 143 nt of the 3' region of ORF 5 (Fig. 2, Fig. 4d) was subcloned into pBS (-) cut with SalI and HindIII. The subclone was digested with SalI and 3' end-labelled resulting in a 3670 nt fragment (3193 nt vector plus 477 nt insert) (Fig. 4d).

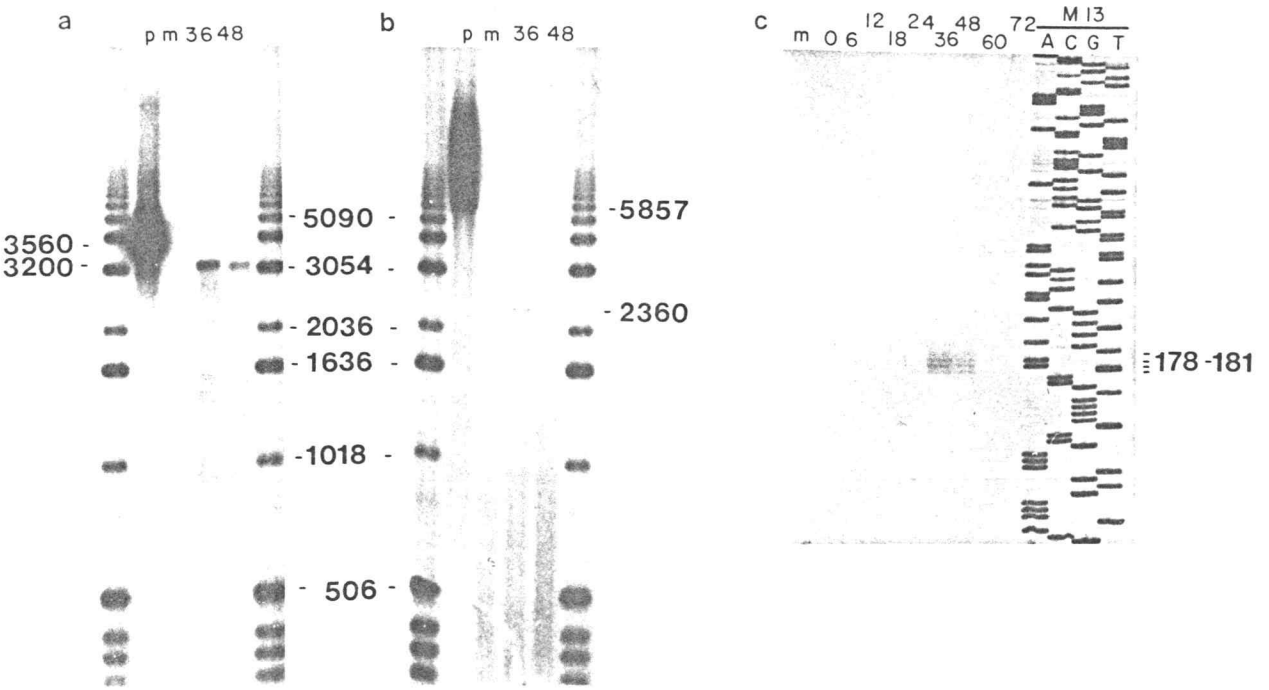
a
p m 36 48
3560
3200
5090
3054
2036
1636
1018
506
b
p m 36 48
5857
2360
c
m 0 6 12 18 24 36 48 60 72
M 13
A C G T
178
181

Figure III.4

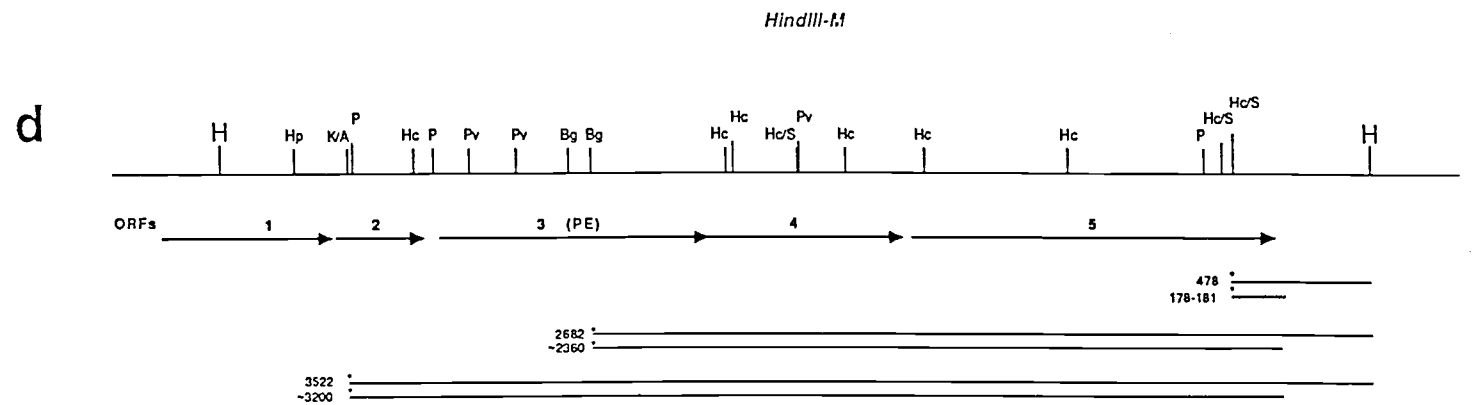

Figure III.4
Continued

Fig. III. 5. Primer extension and Northern analysis of HindIII-M mRNA. a) Primer extension analysis to determine mRNA start sites upstream of ORFs 2-5. For size markers, an M13mp18 sequencing ladder (order ACGT) is present to the right of each primer extension experiment. The numbers to the left indicate the size of the major primer extension products. The numbers at the top indicate the hpi, and 'm' indicates total RNA from a mock infected sample. The samples were analysed on an 8% polyacrylamide, 7M urea gel. b) Northern blot analysis of transcripts from the ORF 5 region. The numbers to the left indicate the location of labelled standards, and the numbers on the right indicate the sizes of major transcripts. This analysis was done using polyA$^+$ RNA collected at 24 hpi electrophoresed on 1.25% agarose, 6% formaldehyde gels. The Northern hybridization probe was produced by cloning a HincII restriction fragment from within ORF 5 (see cross-hatched) into the transcription vector pBS (-) . c) Summary of transcriptional mapping data. The ORFs are duplicated below the restriction map of the HdIII-M region. The verticle lines delineate ORFs relative to the transcripts mapped (arrows). The numbers at the right indicate the size of the mRNAs. Because most of these mRNAs vary over 6 nt due to heterogeneity in the 3′ and 5′ ends, the mRNA sizes have been calculated to the nearest 10 nt.

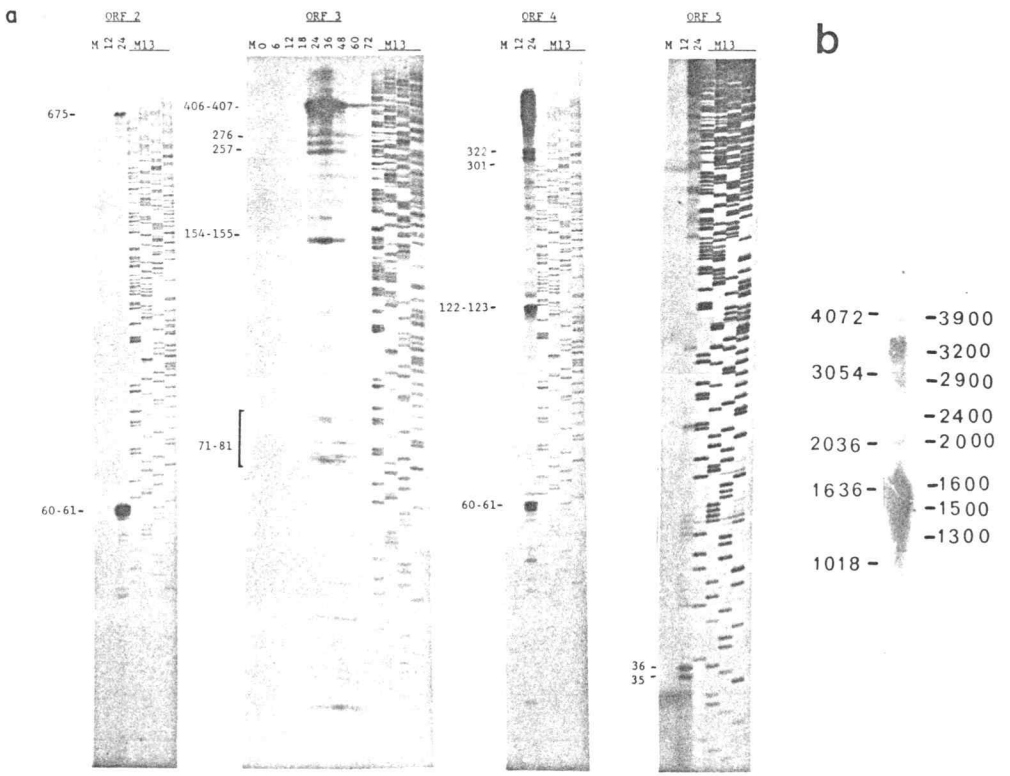
a
ORF 2
M 12 24 M13
675-
60-61-
ORF 3
M 0 6 12 18 24 36 48 60 72 M13
406-407-
276-
257-
154-155-
71-81
ORF 4
M 12 24 M13
322-
301-
122-123-
60-61-
ORF 5
M 12 24 M13
36-
35-
b
4072-
3054-
2036-
1636-
1018-
-3900
-3200
-2900
-2400
-2000
-1600
-1500
-1300

Figure III.5

C

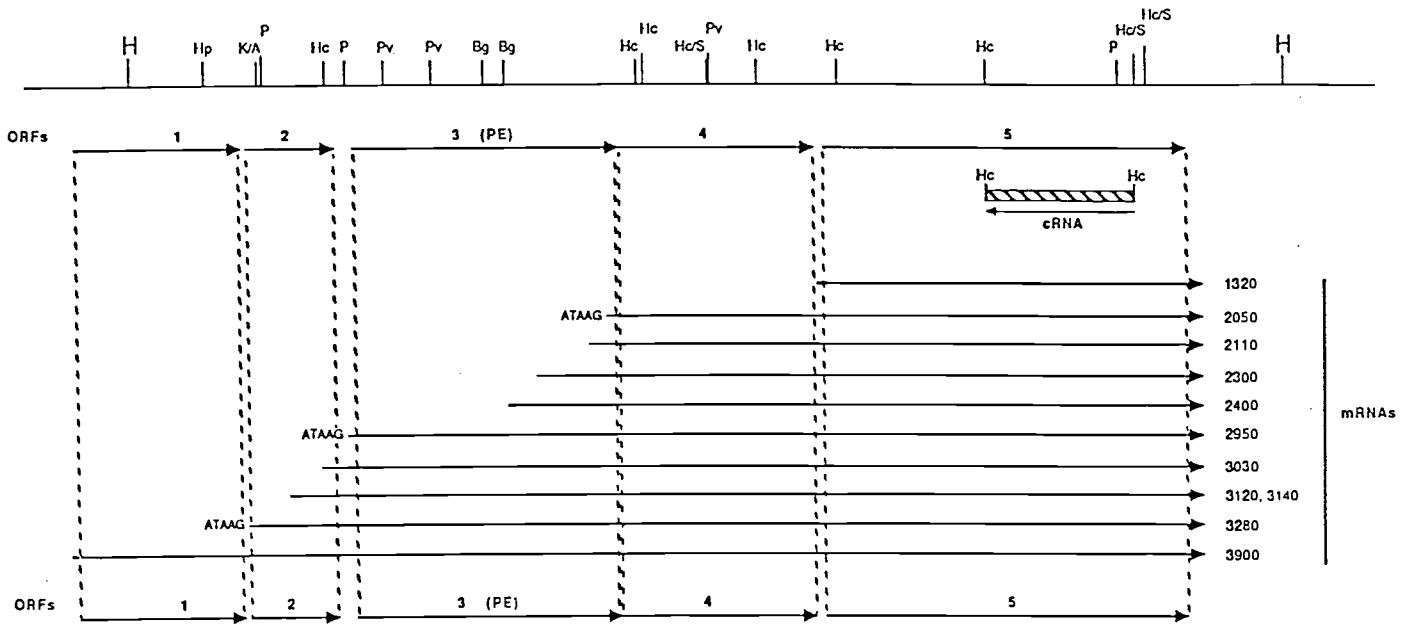

Figure III.5
Continued

Fig. III. 6. Comparison of the predicted amino acid sequences from ORFs 1, 2, 4 and 5 of AcMNPV and OpMNPV. Comparison of ORF 3 is described elsewhere (Gombart et al., 1989). The dots indicate identical amino acids. The location of the putative transposable element in ORF 1 of AcMNPV is designated by the vertical arrow after amino acid 101. The AcMNPV ORF 1 sequence was predicted from the report of Oellig et al (1987) and Whitford et al, (1989). Three changes in the sequence of Oellig et al were introduced to produce the alignment. The sequence of Whitford et al (1989) contains a G inserted after nt 8 of the Oellig et al sequence. In addition, the G at nt 106 and C at nt 168 were deleted from the sequence of Oellig et al. The MW of each protein is indicated at the end of each amino acid sequence. The protein alignment was done using gap penalties of 1,2,3,and 2 for ORFs 1,2,4,and 5 respectively.

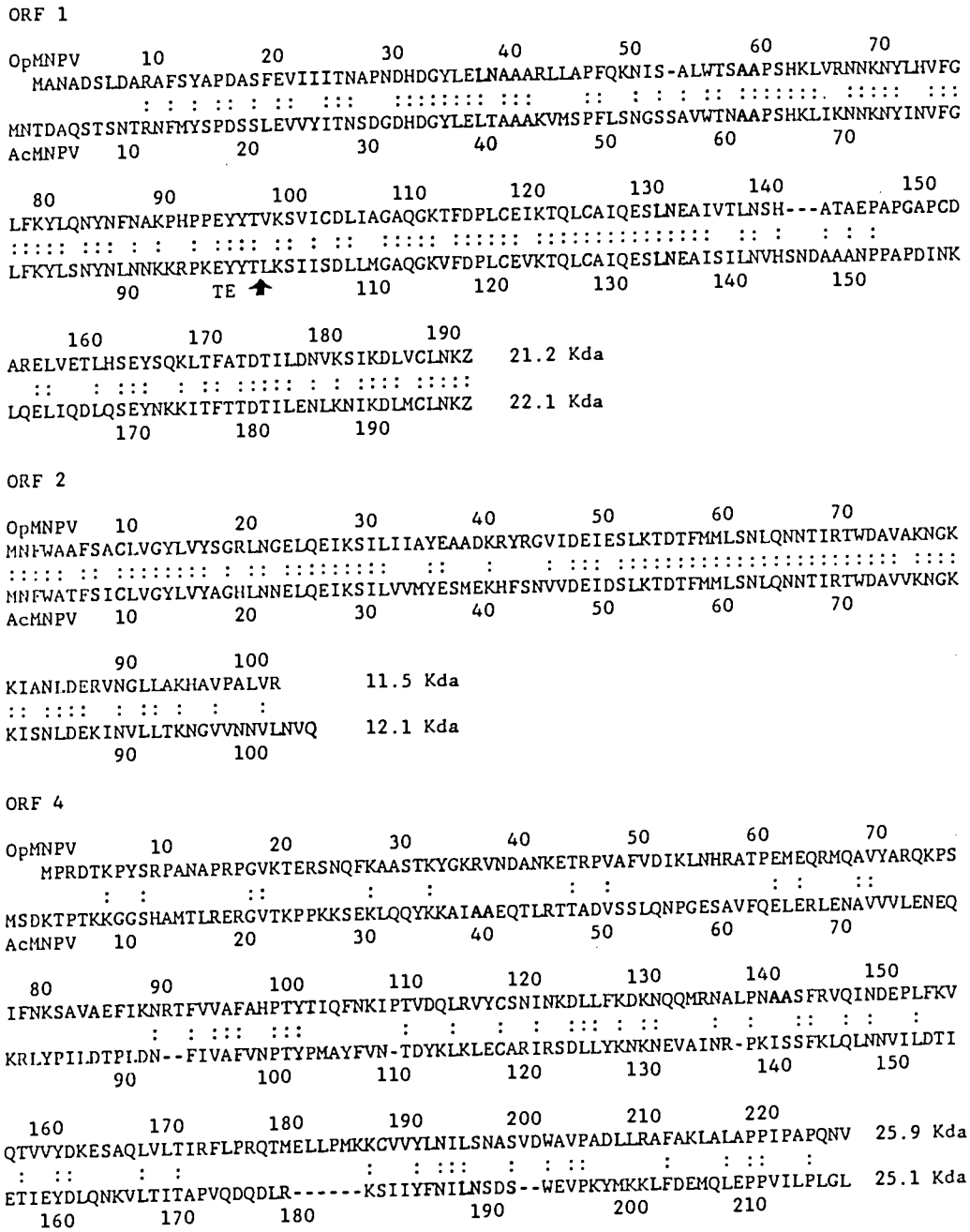
ORF 1
OpMNPV
AcMNPV
21.2 Kda
22.1 Kda
ORF 2
OpMNPV
AcMNPV
11.5 Kda
12.1 Kda
ORF 4
OpMNPV
AcMNPV
25.9 Kda
25.1 Kda

Figure III.6

ORF 5

```
OpMNPV   10         20         30         40         50         60         70
MHAPLTAEQRDVYDKYKFATYARSVALTRAQLDQWRDNKVIVPEPVSRAETLRVEAATRGQSKNALWNLLRLDRSTASRS
: : :: ::     :::: :     :  ::: :: :: : : :  ::: :::: :::::::: :: :::::: ::: :
MFASLTSEQKLLLKKYKFNNYVKTIELSQAQLAHWRSNKDIQPKPLDRAEILRVEKATRGQSKNELWTLLRLDRNTASAS
AcMNPV   10         20         30         40         50         60         70

            90         100        110        120        130        140        150
SG--GVALRSSALAFGNAQENRLKLANGELFERLGRLAAERAGGPVAETVLDCGMFISAFGLHSASPDAYFAMADGSCVP
:   :  :   :: ::::::   :  ::                  : :::::::: :  ::: :::::::  :::   :
SNSSGNMLQRPALLFGNAQESHVKETNGIMLDHMREIIESKIMSAVVETVLDCGMFFSPLGLHAASPDAYFSLADGTWIP
         90        100        110        120        130        140        150

 160        170        180        190        200        210        220        230
VEIKCPFNYRDTTVDQMRLELGKANRKYRVKHTALLVNKAGPAQFEVVKTHDHYRQMQRQMYVMRNAPVCFYVVRFKHNL
:::::: ::::::: ::: :::  :::::::::::::::: :  ::: :::  :: :::::::: :::  :::: :: ::
VEIKCPYNYRDTTVEQMRVELGNGNRKYRVKHTALLVNKKGTPQFEMVKTDAHYKQMQRQMYVM-NAPMGFYVVKFKQN
         170        180        190        200        210        220        230

 240        250        260        270        280        290        300        310
VALAVPRDDDFGRKEAAAEGAAFVAFATENAGRVQFKRGDRRRASFAQNAADHGYNAAQVDALVRRGLYLSYGQLRCGHC
:   ::::  :: ::   :  : :::: ::          : :: ::       : :      :: : :: :: :: : :  :
VVVSVPRDETFGNKELSTENNAYVAFAVENSNGARYQGADKRRLSFKTHSGNHNYSGQEIDAMVDRGIYLDYGHLKGAYG
240        250        260        270        280        290        300        310

 320        330        340        350        360        370        380        390
DAFALDGPRAFELAMARPHEQGDGLALQEHEFDNVAFLDFTKRYTSLVDKRGD--DARALRVDGFYVDDAGAVKTFGGGV
: :  :          : :  :    :    :::    :  ::  ::         ::  :   : :    :  ::::::
D-FSSDSRETGDSVLKREHTNGKSFNLKHKNFDNPTYFDYVKRLQSLLKSHHFRNDAKTLAYFGYYLTHTGTLKTFGGGS
320        330        340        350        360        370        380        390

   400        410        420
HGSNASRR-HLPTGSYYLAMGVNKIQNNM  47.3 Kda
  :      ::  : :::
QNSSPTKHDHLNDGVYYLEIK          48.3 Kda
 400        410
```

Figure III.6
Continued

Fig. III. 7. Comparison of the OpMNPV HindIII M-Q gene organization with AcMNPV. a) HindIII restriction enzyme map of OpMNPV genome. The location of polyhedrin (PH) and p39 are indicated. b) Organization of the ORFs in the OpMNPV HindIII M-Q region. The five ORFs reported in this study are located immediately upstream of the genes for p26, p10 and p74. The inserts below this map indicate the major differences between the OpMNPV and AcMNPV genomes in this region. The location of the retrotransposon (TE-D) reported by Miller and Miller (1982) is indicated. The AcMNPV sequence used in this analysis is from Kuzio et al., 1984; Liu et al., 1986; Friesen and Miller, 1987; and Oellig et al., 1987. The OpMNPV sequence used in this analysis is from Leisy et al, 1986; Bicknell et al, 1987; and this study.

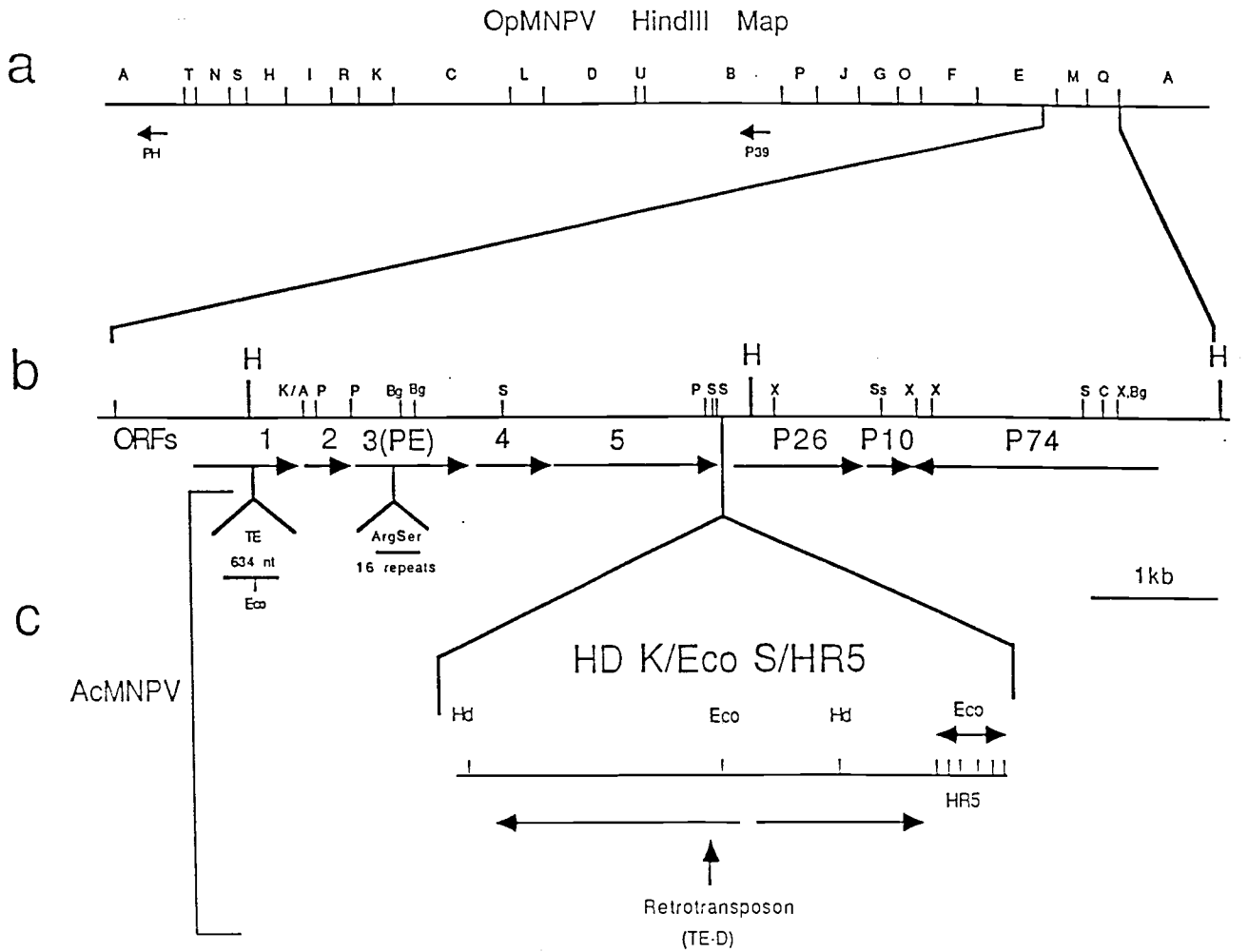
OpMNPV HindIII Map
a
A T N S H I R K C L D U B P J G O F E M Q A
PH
P39
b
H H H
K/A P P Bg Bg S P S S X Ss X X S C X,Bg
ORFs 1 2 3(PE) 4 5 P26 P10 P74
TE
634 nt
Eco
ArgSer
16 repeats
1kb
c
AcMNPV
HD K/Eco S/HR5
Hd Eco Hd Eco
HR5
Retrotransposon
(TE-D)

Figure III.7

REFERENCES

Beames, B., & Summers, M.D. (1988). Comparisons of host cell DNA insertions and altered transcription at the site of insertions in few polyhedra baculovirus mutants. Virology 162, 206-220.

Bicknell, J.N., Leisy, D.J., Rohrmann, G.F., & Beaudreau, G.S. (1988). Comparison of the p26 gene region of two baculoviruses. Virology 161 , 589-592.

Blissard, G., Russell, R., Rohrmann, G.F., & Beaudreau, G.S. Nucleotide sequence and expression of the gene encoding p39, a major structural protein of the multicapsid nuclear polyhedrosis virus of Orgyia pseudotsugata. Virology 168, 354-362.

Burgess, S. (1977). Molecular weights of lepidopteran baculovirus DNAs: derivation by electron microscopy. Journal of General Virology 37, 501-510.

Carstens, E.B. (1987). Identification and nucleotide sequence of the regions of Autographa californica nuclear polyhedrosis virus genome carrying insertion elements derived from Spodoptera frugiperda. Virology 161, 8-17.

Crook, N.E. (1981). A comparison of the granulosis viruses from Pieris brassicae and Pieris rapae. Virology 115, 173-181.

Feinberg, A.P. & Vogelstein, B. (1984). A technique for radiolabelling DNA restriction fragments to high specific activity. Analytical Biochemistry 132, 6-13.

Favaloro, J., Treisman, R., & Kamen, R. (1980). Transcriptional maps of polyoma virus-specific RNA: analysis by two dimensional nuclease S1 gel mapping. Methods in Enzymology 65, 718-749.

Fraser, M. J., G. E. Smith, & M. D. Summers. (1983). Aquisition of host cell DNA sequences by Baculoviruses; Relationships between host DNA insertions and FP mutants of Autographa californica and Galleria mellonella nuclear polyhedrosis virus. Journal of Virology 47, 287-300.

Friesen, P.D., Rice, W.C., Miller, D.W., & Miller, L.K. (1986). Bidirectional transcription from a solo long terminal repeat of the retrotransposon TED; symmetrical RNA start sites. Molecular and Cellular Biology 6, 1599-1607.

Friesen, P.D. & Miller, L.K. (1987). Divergent transcription of early 35- and 94-kilodalton protein genes encoded by the HindIII K genome fragment of the baculovirus Autographa californica nuclear polyhedrosis virus. Journal of Virology 61, 2264-2272.

Gombart, A.F., Pearson, M.N., Rohrmann, G.F., & Beaudreau, G.S. A baculovirus polyhedral envelope-associated protein: Genetic location, nucleotide sequence and immunocytochemical characterization. Virology, in press.

Guarino, L.A. & Summers, M.D. (1986). Functional mapping of a trans-activating gene required for expression of a baculovirus delayed-early gene. Journal of Virology 57, 563-571.

Henikoff, S. (1984). Unidirectional digestion with exonuclease III creates targeted breakpoints for DNA sequencing. Gene 28, 351-359.

Kozak, M. (1986). Point mutations define a sequence flanking the AUG initator codon that modulates translation by eukaryotic ribosomes. Cell 44, 283-292.

Kuzio, J. D., Rohel, Z., Curry, C.J., Krebs, A., Carstens, E.B. & Faulkner, P. (1984). Nucleotide sequence of the p10 polypeptide gene of Autographa californica nuclear polyhedrosis virus. Virology 139, 414-418.

Leisy, D.J., Rohrmann, G.F., & Beaudreau, G.S. (1984). Conservation of genome organization in two multicapsid nuclear polyhedrosis viruses. Journal of Virology 52, 699-702.

Leisy, D.J., Rohrmann, G.F., Nesson, M., & Beaudreau, G.S. (1986). Nucleotide sequence and transcriptional mapping of the p10 gene region of the Orgyia pseudotsugata multicapsid nuclear polyhedrosis virus. Virology 153, 157-167.

Lewin, B. (1985). Genes. Second Ed. John Wiley & Sons. New York.

Liu, A, Qin, J., Rankin, C., & Weaver, R. R. (1986). Nucleotide sequence of a portion ofthe Autographa californica nuclear polyhedrosis virus genome containing the Eco Rl site-rich region (hr5) and a new open reading frame overlapping the p10 gene. Virology 67, 2565-2570.

Maniatis, T., Fritsch, E.F., & Sambrook, J. (1982). Molecular cloning: a laboratory manual. Cold Spring Harbor Laboratory, Cold Spring Harbor,N.Y.

Martignoni, M.E., & Iwai, P.J. (1986). A Catalog of viral Diseases of Insects, Mites, and Ticks. Fourth Ed. USDA Forest Service PNW-195.

Miller, D. W., & Miller, L. K. (1982). A virus mutant with an insertion of a copia-like transposable element. Nature (London) 299, 562-564.

Oellig, C., Happ, B., Muller, T., & Doerfler, W. (1987).

Overlapping sets of viral RNAs reflect the array of polypeptides in the EcoR1 J and N Fragments (map positions 81.2 to 85.0) of the Autographa californica nuclear polyhedrosis virus. Journal of Virology 61, 3048-3057.

Possee, R.D., & Howard, S.C. (1987). Analysis of the polyhedrin gene promoter of the Autographa californica nuclear polyhedrosis virus. Nucleic Acids Research 15, 10233-10248.

Quant-Russell, R.L., Pearson, M.N., Rohrmann, G.F., & Beaudreau, G.S. (1987). Characterization of baculovirus p10 synthesis using monoclonal antibodies. Virology 160, 9-19.

Rohrmann, G.F., (1986). Polyhedrin Structure. Journal of General Virology 67, 1499-1513.

Rohrmann, G.F., Martignoni, M.E., & Beaudreau, G.S. (1982). DNA sequence homology between Autographa californica and Orgyia pseudotsugata nuclear polyhedrosis viruses. Journal of General Virology 62,. 137-143.

Schafer, M.P., Rohrmann, G., Heine, U. & Beaudreau, G.S. (1979). DNA from two Orgyia pseudotsugata baculoviruses: Molecular weight determination by means of electron microscopy and restriction endonuclease analysis. Virology 95, 176-184.

Sanger, F., Coulson, A.R., Barrell, B.G., Smith, A.J.H. & Roe, B.A. (1980). Cloning in single stranded bacteriophage as an aid to rapid DNA sequencing. Journal of Molecular Biology 143, 161-178.

Sharp, P.A., Berk, A.J., & Berget, S.A. (1980). Transcription maps of Adenovirus. Methods in Enzymology 65, 750-768.

Smith, G. E., & Summers, M.D. (1982). DNA homology among subgroup A,B and C baculoviruses. Virology 123, 393-406.

Whitford, M., Stewart, S., Kuzio, J., and Faulkner, P. (1989). Identification and sequence analysis of a gene encoding gp67 an abundant envelope glycoprotein of the baculovirus, Autographa californica nuclear polyhedrosis virus. Journal of Virology, in press.

Whitt, M.A. & Manning, J.S. (1988). A phosphorylated 34-kDa protein and a subpopulation of polyhedrin are thiol linked to the carbohydrate layer surrounding a baculovirus occlusion body. Virology 163, 33-4

BIBLIOGRAPHY

Beames, B., & Summers, M.D. (1988). Comparisons of host cell DNA insertions and altered transcription at the site of insertions in few polyhedra baculovirus mutants. Virology 162, 206-220.

Bicknell, J.N., Leisy, D.J., Rohrmann, G.F., and Beaudreau, G.S. (1988). Comparison of the p26 gene region of two baculoviruses. Virology 161 , 589-592.

Blissard, G., Russell, R., Rohrmann, G.F., & Beaudreau, G.S. (1989). Nucleotide sequence and expression of the gene encoding p39, a major structural protein of the multicapsid nuclear polyhedrosis virus of Orgyia pseudotsugata. Virology 168, 354-362.

Burgess, S. (1977). Molecular weights of lepidopteran baculovirus DNAs: derivation by electron microscopy. Journal of General Virology 37, 501-510.

Carstens, E.B. (1987). Identification and nucleotide sequence of the regions of Autographa californica nuclear polyhedrosis virus genome carrying insertion elements derived from Spodoptera frugiperda. Virology 161, 8-17.

Chisholm, G.E. and Henner, D.J. (1988). Multiple early transcripts and splicing of the Autographa californica nuclear polyhedrosis virus IE-1 gene. Journal of Virology 62, 3193-3200.

Crook, N.E. (1981). A comparison of the granulosis viruses from Pieris brassicae and Pieris rapae. Virology 115, 173-181.

Dieckmann, C.L. and Tzagoloff, A. (1985). Assembly of the mitochondrial membrane system. Journal of Biological Chemistry 260, 1513-1520.

Erlandson, M.A. and Carstens, E.B. (1983). Mapping early transcription products of Autographa californica nuclear polyhedrosis virus. Virology 126, 398-402.

Favaloro, J., Treisman, R., & Kamen, R. (1980). Transcriptional maps of polyoma virus-specific RNA: analysis by two dimensional nuclease S1 gel mapping. Methods in Enzymology 65, 718-749.

Feinberg, A.P. and Vogelstein, B. (1984). A technique for radiolabelling DNA restriction fragments to high specific activity. Analytical Biochemistry 132, 6-13.

Fraser, M. J., G. E. Smith, & M. D. Summers. (1983). Aquisition of host cell DNA sequences by Baculoviruses; Relationships between host DNA insertions and FP mutants of Autographa californica and Galleria mellonella nuclear polyhedrosis virus. Journal of Virology 47, 287-300.

Friesen, P.D. and Miller, L.K. (1985). Temporal regulation of baculovirus RNA: overlapping early and late transcripts. Journal of Virology 54, 392-400.

Friesen, P.D. and Miller, L.K. (1986). The regulation of baculovirus gene expression. Current Topics in Microbiology and Immunology 131, 31-49.

Friesen, P.D., Rice, W.C., Miller, D.W., & Miller, L.K. (1986). Bidirectional transcription from a solo long terminal repeat of the retrotransposon TED; symmetrical RNA start sites. Molecular and Cellular Biology 6, 1599-1607.

Friesen, P.D. & Miller, L.K. (1987). Divergent transcription of early 35- and 94-kilodalton protein genes encoded by the HindIII K genome fragment of the baculovirus Autographa californica nuclear polyhedrosis virus. Journal of Virology 61, 2264-2272.

Gombart, A.F., Pearson, M.N., Rohrmann, G.F., & Beaudreau, G.S. (1989). A baculovirus polyhedral envelope-associated protein: Genetic location, nucleotide sequence and immunocytochemical characterization. Virology, in press.

Granados, R.R. (1980). Infectivity and mode of action of baculoviruses. Biotechnology and Bioengineering 22, 1377-1405.

Granados, R. R. and Williams, K.K. (1986). In vivo infection and replication of baculoviruses. pp. 89-108. In: Granados, R.R. and Federichi, B.A. eds. The biology of baculoviruses Volume I biological properties and molecular biology. CRC Press, Inc., Boca Raton, Florida USA.

Guarino, L.A. & Summers, M.D. (1986). Functional mapping of a trans-activating gene required for expression of a baculovirus delayed-early gene. Journal of Virology 57, 563-571.

Hager, D.A and Burgess, R.R. (1980). Elution of proteins from sodium dodecyl sulfate-polyacrylamide gels, removal of sodium dodecyl sulfate, and renaturation of enzymatic activity: results with sigma subunit of *Escherichia coli* RNA polymerase, wheat germ DNA topoisomerase, and other enzymes. Analytical Biochemistry 109, 76-86.

Henikoff, S. (1984). Unidirectional digestion with exonuclease III creates targeted breakpoints for DNA sequencing. Gene 28, 351-359.

Kleid, D.G., Yanasura, D., Small, B., Dowbenko, D., Moore, D.M., Grubman, M.J., McKercher, P.D., Morgan, D.O., Robertson, B.H., and Bachrach, H.L. (1981). Cloned viral protein for foot-and-mouth disease: responses in cattle and swine. Science 241, 1125-1129.

Kozak, M. (1986). Point mutations define a sequence flanking the AUG initator codon that modulates translation by eukaryotic ribosomes. Cell 44, 283-292.

Kuzio, J., Rohel, D.Z., Curry, C.J., Krebs, A., Carstens, E.B. and Faulkner, P. (1984). Nucleotide sequence of the p10 polypeptide gene of *Autographa californica* nuclear polyhedrosis virus. Virology 139, 414-418.

Kyte, J. and Doolittle, R.F. (1982). A simple method for displaying the hydropathic character of a protein. Journal of Molecular Biology 157, 105-132.

Laemmli, U.K. (1970). Cleavage of structural proteins during the assembly of the head of bacteriophage T4. Nature (London) 227, 680-685.

Leisy, D.J., Rohrmann, G.F., Beaudreau, G.S. (1984). Conservation of genome organization in two multicapsid nuclear polyhedrosis viruses. Journal of Virology 52, 699-702.

Leisy, D.J., Rohrmann, G.F., Nesson, M., and Beaudreau, G.S. (1986). Nucleotide sequence and transcriptional mapping of the p10 gene region of the *Orgyia pseudotsugata* multicapsid nuclear polyhedrosis virus. Virology 153, 157-167.

Lewin, B. (1985). Genes. Second Ed. John Wiley & Sons. New York.

Liu, A, Qin, J., Rankin, C., & Weaver, R. R. (1986). Nucleotide sequence of a portion ofthe Autographa californica nuclear polyhedrosis virus genome containing the Eco R1 site-rich region (hr5) and a new open reading frame overlapping the p10 gene. Virology 67, 2565-2570.

Lote, C.J. and Weiss, J.B. (1971). Identification of digalactosylcysteine in a glycopeptide isolated from urine by a new preparative technique. FEBS Letters 16, 81-85.

Lubbert, H. and Doerfler, W. (1984a). Mapping of early and late transcripts encoded by the Autographa californica nuclear polyhedrosis virus genome: Is viral RNA spliced? Journal of Virology 50, 497-506.

Lubbert, H. and Doerfler, W. (1984b). Transcription of overlapping sets of RNAs from the genome of Autographa californica nuclear polyhedrosis virus: A novel method for mapping RNAs. Journal of Virology 52, 255-265.

Maniatis, T., Fritsch, E.F., and Sambrook, J. (1982). Molecular cloning: a laboratory manual. Cold Spring Harbor Laboratory, Cold Spring Harbor, N.Y.

Martignoni, M.E., & Iwai, P.J. (1986). A Catalog of viral Diseases of Insects, Mites, and Ticks. Fourth Ed. USDA Forest Service PNW-195.

McClintock, J.T., Dougherty, E.M., and Weiner, R.M. (1986). Protein synthesis in gypsy moth cells infected with a nuclear polyhedrosis virus of *Lymantria dispar*. Virus Research 5, 307-322.

Miller, D. W., & Miller, L. K. (1982). A virus mutant with an insertion of a copia-like transposable element. Nature (London) 299, 562-564.

Minion, F.C., Coons, L.B., and Broome, J.R. (1979). Characterization of the polyhedral envelope of the nuclear polyhedrosis virus of *Heliothis virescens*. Journal Invertebrate Pathology 34, 303-307.

Oellig, C., Happ, B., Muller, T., & Doerfler, W. (1987). Overlapping sets of viral RNAs reflect the array of polypeptides in the EcoRl J and N Fragments (map positions 81.2 to 85.0) of the *Autographa californica* nuclear polyhedrosis virus. Journal of Virology 61, 3048-3057.

Pearson, M.N., Quant-Russell, R.L., Rohrmann, G.F., and Beaudreau, G.S. P39, a major baculovirus structural protein: Immunocytochemical characterization and genetic location. Virology 167, 407-413.

Possee, R.D., & Howard, S.C. (1987). Analysis of the polyhedrin gene promoter of the Autographa californica nuclear polyhedrosis virus. Nucleic Acids Research 15, 10233-10248.

Quant, R.L., Pearson, M.N., Rohrmann, G.F., and Beaudreau, G.S. (1984). Production of polyhedrin monoclonal antibodies for distinguishing two *Orgyia pseudotsugata* baculoviruses. Applied Environmental Microbiology 48, 732-736.

Quant-Russell, R.L., Pearson, M.N., Rohrmann, G.F., and Beaudreau, G.S. (1987). Characterization of baculovirus p10 synthesis using monoclonal antibodies. Virology 160, 9-19.

Rankin, C., Ladin, B.F., and Weaver, R.F. (1986). Physical mapping of temporally regulated overlapping transcripts in the region of the 10K protein gene of Autographa californica nuclear polyhedrosis virus. Journal of Virology 57, 18-27.

Rohrmann, G.F., Martignoni, M.E., & Beaudreau, G.S. (1982). DNA

sequence homology between Autographa californica and Orgyia pseudotsugata nuclear polyhedrosis viruses. Journal of General Virology 62, 137-143.

Rohrmann, G.F., (1986). Polyhedrin Structure. Journal of General Virology 67, 1499-1513.

Sanger, F., Coulson, A.R., Barrell, B.G., Smith, A.J.H. and Roe, B.A. (1980). Cloning in single stranded bacteriophage as an aid to rapid DNA sequencing. Journal of Molecular Biology 143, 161-178.

Schafer, M.P., Rohrmann, G., Heine, U. & Beaudreau, G.S. (1979). DNA from two Orgyia pseudotsugata baculoviruses: Molecular weight determination by means of electron microscopy and restriction endonuclease analysis. Virology 95, 176-184.

Sharp, P.A., Berk, A.J., & Berget, S.A. (1980). Transcription maps of Adenovirus. Methods in Enzymology 65, 750-768.

Smith, G. E., & Summers, M.D. (1982). DNA homology among subgroup A,B and C baculoviruses. Virology 123, 393-406.

Spindler, K.R., Rosser, D.S.E. and A.J.Berk. (1984). Analysis of adenovirus transforming proteins from early regions 1A and 1B with antisera to inducible fusion antigens produced in *Escherichia coli*. Journal of Virology 49, 132-141.

Summers, M.D. (1971). Electron microscope observations on granulosis virus entry, uncoating and replication process during infection of the cells of Trichoplusia ni. Journal of Ultrastructural Research 35, 606-625.

Tollefson, A.E. and Wold, W.S.M. (1988). Identification and gene mapping of a 14,700-molecular-weight protein encoded by region E3 of group C adenoviruses. Journal of Virology 62, 33-39.

Van der Wilk, F., Van Lent, J.W.M. and Vlak, J.M. (1987). Immunogold detection of polyhedrin, p10 and virion antigens in Autographa californica nuclear polyhedrosis virus-infected Spodoptera frugiperda cells. Journal of General Virology 68, 2615-2623.

Vlak, J.M., & Rohrmann, G.F. 1985. The Nature of Polyhedrin. Pp. 489-544. In: Maramorosch, K. and Sherman, K.E. eds. Viral Insecticides for Biological Control. Academic Press, Orlando, FL USA.

Volkman, L.E. (1986). The 64K envelope protein of budded *Autographa californica* nuclear polyhedrosis virus. Current Topics in Microbiology and Immunology 131, 103-117.

Volkman, L.E. and Goldsmith, P.A. (1984). Budded Autographa californica NPV 64K protein: further biochemical analysis and

effects of postimmunoprecipitation sample preparation conditions. Virology 139, 295-302.

Volkman, L.E. and Goldsmith, P.A. (1985). Mechanism of neutralization of budded Autographa californica nuclear polyhedrosis virus by a monoclonal antibody: inhibition of entry by adsorptive endocytosis. Virology 143, 185-195.

Weiss, J.B., Lote, C.J., and Bobinski, H. (1971). New low molecular weight glycopeptide containing triglucosylcysteine in human erythrocyte membrane. Nature New Biology 234, 25-26.

Whitford, M., Stewart, S., Kuzio, J., and Faulkner, P. (1989). Identification and sequence analysis of a gene encoding gp67 an abundant envelope glycoprotein of the baculovirus, Autographa californica nuclear polyhedrosis virus. Journal of Virology, in press.

Whitt, M.A. and Manning, J.S. (1988). A phosphorylated 34-kDa protein and a subpopulation of polyhedrin are thiol linked to the carbohydrate layer surrounding a baculovirus occlusion body. Virology 163, 33-42.

Wilson, M.E., Mainprize, T.H., Friesen, P.D., and Miller, L.K. (1987). Location, transcription, and sequence of a baculovirus gene encoding a small arginine-rich polypeptide. Journal of Virology 61, 661-666.